3D Self-Supporting Porous Magnetic Assemblies for Water Remediation and Beyond

*Ran Du, Qiuchen Zhao, Zhe Zheng, Wenping Hu, and Jin Zhang**

In the past few years, three-dimensional self-supporting porous magnetic assemblies (3D-SPMAs) have emerged as a new research area in materials science because of their combined features of three-dimensional self-supporting porous assemblies (3D-SPAs) and magnetic materials. Due to these attributes, 3D-SPMAs gain numerous tempting properties such as magnetism-induced actuating, magnetic shape memory effects, and alternative magnetic field (AMF) induced heat generation, showcasing huge potential in diverse applications stretching over water remediation, actuators, biomedical therapy, etc. Especially, 3D-SPMAs displayed eminent potential in water remediation for their large processing capacity, remote controllability, and magnetic-field-mediated wettability. With the rising interest in 3D-SPAs, the increasing understanding of magnetic materials, and the flourish of materials preparation technique, an upsurge has appeared in 3D-SPMAs and thus managing them a class of emerging and promising functional materials. However, currently there are rarely review papers concerning 3D-SPMAs. In this light, this review aims to express a comprehensive overview of this young field and fuel further innovations for preparation methods and practical applications of 3D-SPMAs. The focus is placed on the synthetic strategies and applications especially in water remediation. The potential opportunities and challenges are also discussed.

1. Introduction

It is fundamentally interesting and practically useful to marry magnetism with materials on macroscopic dimensions, from which a wealth of applications could be achieved, especially for water remediation. Water remediation, mainly including selective oil adsorption, oil/water separation, removal of dyes and heavy-metal ions, have evoked elevated public concerns due to the increasingly aggravated water pollution throughout the world from the discharge of industrial effluents and oil spill accidents.[1,2] In addition, the purified water and collected pollution (e.g., crude oil, methanol) by water remediation are also pivotal sources for preparing energetic substances (e.g., H_2) and generating energy via the process of water splitting, thermal power generation, discharging of fuel cells, etc. To address these problems, three-dimensional self-supporting porous assemblies (3D-SPAs) with monolithic features and special wettability (e.g., hydrophobicity/oleophilicity, hydrophilicity/oleophobicity, and underwater oleophobicity/hydrophilicity) have become rising stars owing to their assorted attractive features, such as multiple functions (e.g., capable of both selective oil uptake and oil/water separation), large processing abilities, and easy handling attribute.[3–5] A series of 3D-SPAs based on commercial polymer foams/sponges/fibers,[2,4,6–9] carbon materials,[10–15] microporous polymers,[16,17] copper foams,[5,18] polydimethylsiloxane,[19] and hydrogels[20,21] have been developed in last few years (**Figure 1**). For example, Wu et al.[7] reported a hydrophobic graphene oxide (GO) coated polyurethane (PU) foam for oil/water separation with high efficiency. Wu and co-workers[14] fabricated ultralight spongy graphene by solvothermal reaction of GO in alcohol, showing an impressive adsorption capacity over 1000 times for pump oil, which is over three order of magnitude larger than conventional used activated carbon. We have

R. Du, Q. C. Zhao, Z. Zheng, Prof. J. Zhang
Center for Nanochemistry
Peking University
Beijing 100871, P.R. China
E-mail: jinzhang@pku.edu.cn
R. Du, Q. C. Zhao, Z. Zheng, Prof. J. Zhang
Beijing National Laboratory for Molecular Sciences
Peking University
Beijing 100871, P.R. China
R. Du, Q. C. Zhao, Z. Zheng, Prof. J. Zhang
Key Laboratory for the Physics
and Chemistry of Nanodevices
Peking University
Beijing 100871, P.R. China
R. Du, Q. C. Zhao, Z. Zheng, Prof. J. Zhang
State Key Laboratory for Structural Chemistry
of Unstable and Stable Species
College of Chemistry and Molecular Engineering
Peking University
Beijing 100871, P.R. China
Z. Zheng, Prof. W. P. Hu
Department of Chemistry
School of Sciences
Tianjin University
Tianjin 300072, P. R. China

DOI: 10.1002/aenm.201600473

developed potential-responsive conducting polymer hydrogels, showing reasonable performance for the removal of several dyes.[20,21] Very recently, copper foams and melamine foams modified with well-defined microstructures have also been fabricated by our group, exhibiting considerably enhanced water/oil selectivity which grants their high performance in oil/water separation or selective oil adsorption.[4,5] However, big challenge lies in the effective control of the 3D-SPAs, especially in oil adsorption process, which obstructed their handling during transportation, using, and recycling. Additionally, it is also desirable to expand the application territory of 3D-SPAs by imparting new properties.

To enhance the controllability, it is natural to come up with the idea of magnetism integration, which allowed the gathering of materials by magnetic field. In fact, many powder-like magnetic materials, such as magnetic nanoparticles and microparticles, have been widely explored in water remediation or contaminants determination for a long time.[22–26] The main working principle lies in the adsorption of contaminants by using magnetic materials based powders at first, followed by the collection and the regeneration of magnetic powders (MPs). On this basis, a series of magnetism-assisted methods, including magnetic solid phase extraction (MSPE),[27,28] magnetic separations,[29,30] and magnetic sorption[31,32] have been developed in water remediation or contamination determination several decades ago. Detailed mechanism and typical examples can be found in several review articles.[27–31] However, the utilization of MPs suffers from certain inherent problems, such as the easy aggregation of small-size and magnetized particles because of their high free energy, the trade-off between the stability and the adsorption performance, the low oil adsorption capacity, and the difficulty in completely retrieval especially when used in large scale.[32–34] Therefore, the 3D self-supporting porous magnetic assemblies (3D-SPMAs) could be a better choice.

Recently, the subject of 3D-SPMAs has emerged as a burgeoning field that bridges the gap between 3D-SPAs and MPs (**Figure 2**). On the one hand, 3D-SPMAs inherit the monolithic architecture, low density, high surface area, and porous structures of 3D-SPAs, enabling their large processing capacity and facile handling process. On the other hand, they also possess the magnetic properties of MPs, thus allowing their magnetic-driven properties, magnetic-induced heating properties, and magnetic-assisted tunable wettability. Additionally, the 3D substrate can fix the magnetic materials by the covalent or noncovalent interactions on their backbones, thus permanently suppressing the aggregation of magnetic components. Hence, 3D-SPMAs can simultaneously extract advantages of both 3D-SPAs and MPs. Moreover, 3D-SPMAs can also acquire certain novel properties or functions, such as magnetic field induced structures modulation and magnetic shape memory effects.[35–37]

In past few years, a number of 3D-SPMAs based on commercial foams/sponges,[33,34,38–40] carbon material aerogels,[41–43] polymers aerogels,[44,45] and hydrogels[46–50] have been fabricated, showing great promise in water remediation and other applications. These 3D-SPMAs are constructed by either bottom-up assembly of magnetic building blocks or modifying as-existing 3D nonmagnetic networks with magnetic materials. For example, Gui et al.[41] reported magnetic carbon nanotubes (CNTs) sponges with high recyclability by in-situ filling iron nanowires in tubes during chemical vapor deposition (CVD) growth. The obtained magnetic sponges are constructed by the randomly assembled individual magnetic CNTs. In another work, Calcagnile et al.[33] fabricated magnetically driven foams by modifying commercial PU foams with superparamagnetic γ-Fe_2O_3/Fe_3O_4 nanoparticles and polytetrafluoroethylene (PTFE) particles. Both materials have been employed as efficient and remote-controllable adsorbents towards a wide range oils and organic solvents. Apart from the use in water remediation, the 3D-SPMAs could also show certain new functions and applications, especially when combined with other properties such as self-healing properties, electrical conductivity, structural

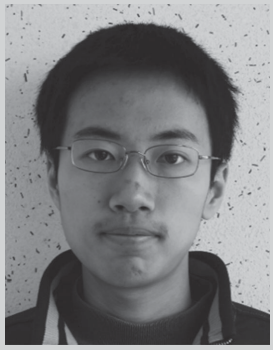

Ran Du received his BSc from Beijing Institute of Technology in 2011. He then joined Prof. Jin Zhang's group to pursue his PhD degree in College of Chemistry and Molecular Engineering, Peking University. His current research interest lies in the synthesis of macroscopic, self-supporting, multifunctional, and porous carbon-based materials for applications in energy, catalysis, and environmental-related fields.

Qiuchen Zhao received his BSc from Peking University in 2013. Since then, he joined Prof. Jin Zhang's group for a five-year PhD program in College of Chemistry and Molecular Engineering, Peking University. His current research is focused on the structurally controlled synthesis of single-walled nanotubes (SWNT), especially on the mechanism of SWNT growth procedures, and the kinetic models during CVD processes.

Jin Zhang received his PhD from Lanzhou University in 1997. After a postdoctoral fellowship at the University of Leeds, UK, he returned to Peking University where he was appointed as Associate Professor (2000) and promoted to Full Professor in 2006. In 2013, he was appointed as Changjiang Professor. His research focuses on the controlled synthesis and spectroscopic characterization of carbon nanomaterials.

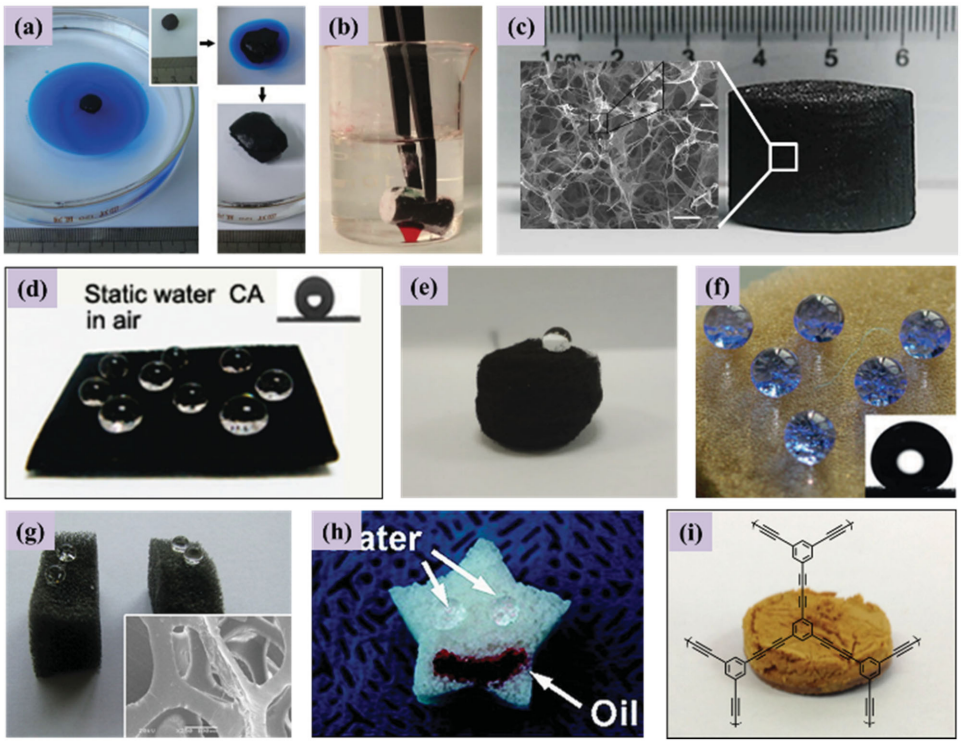

Figure 1. Some representative hydrophobic 3D assemblies: a) carbon nanotubes (CNTs) sponges. Reproduced with permission.[10] Copyright 2010, Wiley-VCH. b) Nitrogen-doped CNTs aerogels. Reproduced with permission.[15] Copyright 2015, Wiley-VCH. c) Spongy graphene. Reproduced with permission.[14] Copyright 2015, Nature Publishing Group. d) Superhydrophobic copper foams. Reproduced with permission.[18] Copyright 2013, Royal Society of Chemistry. e) Carbon fiber aerogels. Reproduced with permission.[8] Copyright 2013, Wiley-VCH. f) Superhydrophobic melamine foams. Reproduced with permission.[2] Copyright 2014, Wiley-VCH. g) Superhydrophobic polyurethane sponges. Reproduced with permission.[9] Copyright 2013, American Chemical Society. h) Polydimethylsiloxane (PDMS) sponges. Reproduced with permission.[19] Copyright 2011, American Chemical Society. i) Conjugated microporous polymers (CMPs) aerogels. Reproduced with permission.[16] Copyright 2015, Wiley-VCH.

anisotropy, etc. Additionally, considering the heat generation of magnetic particles upon an external alternating magnetic field (AMF),[51] more applications, e.g., magnetic-assisted sorbents regeneration, controlled drug release, could be realized.

Therefore, it can be envisaged that the field of 3D-SPMAs will certainly place a great impact on materials science. Thanks to the combination of magnetic properties, porous 3D networks, and free-standing architecture, 3D-SPMAs have found their applications in many fields including water remediation, smart materials, self-healing materials, actuators, controlled drug release, remote therapy, and so on. Although there are a few review articles that partially mention the 3D-SPMAs,[22–26,52,53] to the best of our knowledge, no review has given a systematic and in-depth introduction centering on this subject. Hence, it is crucial to give a comprehensive review on this young yet energetic area, so as to stimulate the studies in 3D-SPMAs, water remediation, and other novel applications. The presented review aims to address a comprehensive introduction of the field of 3D-SPMAs, with the focus on the synthetic strategies of 3D-SPMAs and their applications especially for water remediation. It should be noted that since there is a review centering on the synthesis and applications of magnetic hydrogels for biomedical use,[54] hence the part of magnetic hydrogels in this manuscript will only be briefly stated.

In the second section, certain basic knowledge (magnetic properties, MPs and 3D-SPMAs, and the wettability) are introduced. In the third section, 3D-SPMAs are divided into two main classes according to the medium in 3D networks, i.e., dry 3D-SPMAs (e.g., aerogels, sponges, foams, etc.) and hydrogel-based wet 3D-SPMAs. Corresponding synthetic strategies are summarized and in-depth analyzed. In the fourth section, the mechanism and applications of 3D-SPMAs in water remediation such as remote-control oil uptake, oil/water separation, and dye/heavy-metal-ion removal are exhaustively reviewed, and certain other potential fields that take advantage of the magnetic properties of 3D-SPMAs have also been introduced. Finally, the current research profiles, future opportunities, and challenges of 3D-SPMAs have been concluded in the last part.

2. Fundamental Knowledge

In this section, fundamental knowledge of magnetic materials, features and the comparison of MPs and 3D-SPMAs, and the wettability will be briefly introduced, so as to facilitate the understanding of follow-up sections.

2.1. Magnetic Properties of Materials

The understanding of magnetic properties of materials is essential for the orientated construction of 3D-SPMAs with specific magnetic properties by selecting specific materials and

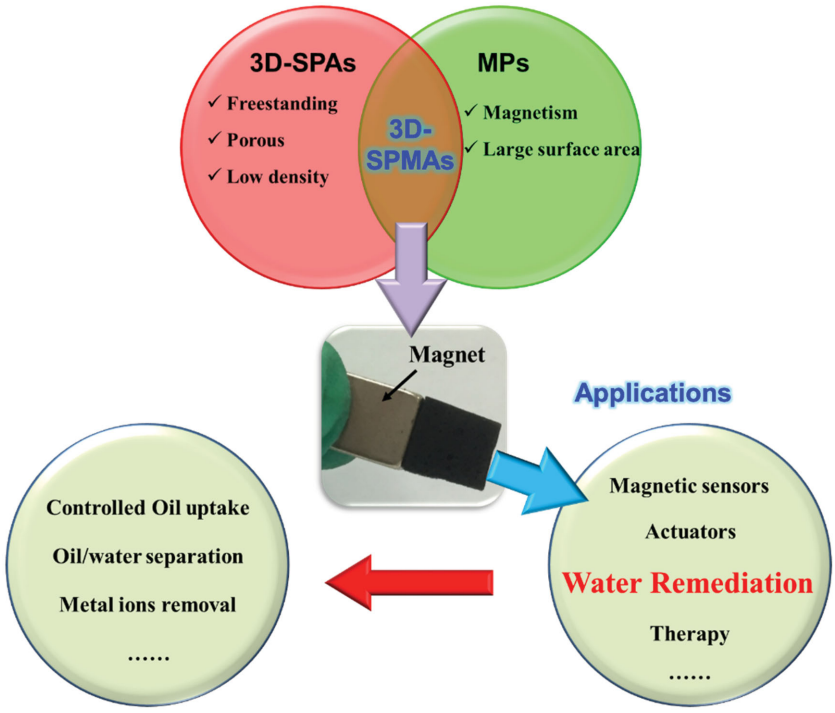

Figure 2. Features and their relationships of 3D-SPAs, MPs, and 3D-SPMAs, and potential applications of 3D-SPMAs.

for facilitating exploring the possible applications of obtained materials.

Magnetism is often generated from unpaired electrons in the orbital shells.[26] On this base, quite a few metal-based materials (Fe, Co, Ni, Fe_3O_4, γ-Fe_2O_3, $CoFe_2O_4$, $Ni_2Co_2O_4$, $Nd_{2x}Fe_{100-3x}B_x$, $BaFe_{12}O_{19}$, $MnFe_2O_4$, Fe_2ZnO_4),[55–59] especially iron-related substances, manifest considerable magnetism. To evaluate the strength of magnetism, saturation magnetization (M_s), characterizing of the saturated magnetization under applied magnetic field, is always adopted. For some examples, the saturation magnetization of bulk iron, cobalt, nickel, Fe_3O_4 and $CoFe_2O_4$ are 221.7, 162, 58.6, 92, and 80 emu g^{-1}, respectively.[60–63] These values serve as a rough basis to design materials with tailored magnetism.

From the aspect of behavior under the applied magnetic field, the magnetic properties can be divided into several categories according to the magnetism, such as ferromagnetism, ferrimagnetism, paramagnetism, and diamagnetism. In most cases, magnetic materials with ferromagnetism and paramagnetism are used for water remediation. For ferromagnetic materials, there are quite a few unpaired electrons exist in materials. In the presence of external magnetic field, magnetic domains in materials tend to be parallel to each other, thus producing significant magnetism that can be retained for a long time even after removal of the applied field. For paramagnetic materials, there are some unpaired electrons in the orbital shells. When subjected in an external magnetic field, materials can be partially magnetized and show positive magnetic moment. However, due to the non-interaction of individual magnetic moment, the net magnetic moment quickly drop to zero when the external field is removed.[27]

The magnetic properties of materials are highly dependent on their sizes. For example, the ferromagnetic materials can be converted to superparamagnetic ones when the particle size is reduced to the size less than ≈10 nm. This is attributed to the weak interactions between small-size individual magnetic particles. In addition, the size reduction always accompanied with considerable alteration of magnetic properties such as saturation magnetization, coercivity, and Curie temperature.[56,64,65] For example, Jun et al.[65] found that the mass magnetization value of water-soluble iron oxide nano-crystal changed from 25 to 102 emu g^{-1} as the size increased from 4 to 12 nm. Therefore, shaping the size of magnetic materials could be used as an alternative strategy to tailor the magnetic properties of materials apart from controlling the chemical compositions.

Besides magnetism, the magnetic components can also serve as the micro-heaters to generate heat when applied with alternating magnetic field (AMF). This AMF-induced heat generation process is always used for biological-related applications. Hence, to avoid the damage of biological tissues, there is certain limitation of frequency and field amplitude. Considering this factor, the heat generation mechanism of magnetic components is always constrained to hysteretic loss.[51] The dissipated energy in the form of heat could be estimated from the magnetization curve (M–H diagram). In detail, the generated heat is characterized by the area enclosed in the hysteresis loops during a magnetization cycle, which is similar to that of energy dissipation in a mechanical compressive curve (stress–strain curve).[66]

2.2. Fundamental Knowledge of Wettability on Solid Surfaces

For water remediation and many other applications (e.g., energy storage), the surface wettability of materials is one of the most important issues needed to be addressed. The comprehension of the origin of wettability and related key factors is the foundation to devise high-performance 3D-SPMAs.

The wettability usually describes the wetting behavior of liquid at solid surfaces, which is determined by the co-effects of chemical nature and roughness of the latter.[67,68] For chemical nature part, the wettability behavior on solid surfaces can be understood by the comparison of solid surface energy and surface tension of liquid. According to one definition, when a drop of water is placed on a flat solid surface, the surface is regarded as hydrophilic surface if the water possess a contact angle less than 65° (Notably, the definition of critical angle to distinguish hydrophilic and hydrophobic surfaces is still controversial).[68,69] In this case, the contact angle and the surface tension follow Young's Equation as follows:

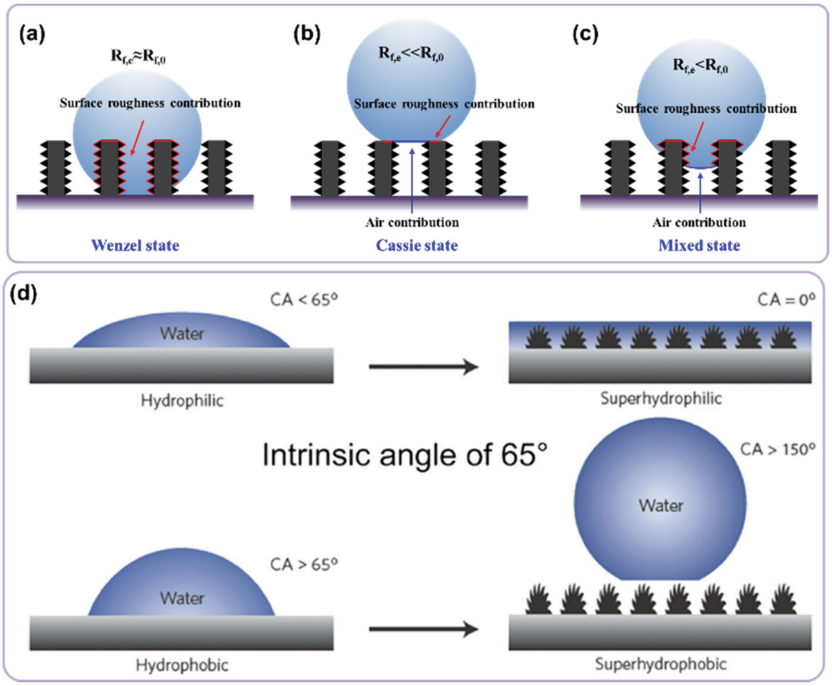

Figure 3. a–c) The demonstration of three state types of a water droplet on rough hydrophobic surfaces. Reproduced with permission.[4] Copyright 2016,Wiley-VCH. d) Illustration of the surface roughness incurred enhanced wettability of water on an intrinsically hydrophilic surface (top) and an intrinsically hydrophobic surface. Reproduced with permission.[68] Copyright 2014, Wiley-VCH.

$$\gamma_{SV} = \gamma_{SL} + \gamma_{LV} \cdot \cos\theta_Y \quad (1)$$

Where γ_{SV}, γ_{SL}, and γ_{LV}, represent the solid/gas, solid/liquid, liquid/gas interface tension, respectively. θ_Y represents the Young's contact angle of water.

However, even for the most hydrophobic flat surface, a contact angle of larger than 120° is nearly impossible to achieve.[70,71] Fortunately, the engineering of surface roughness (SF) provide an effective tactic to break this limitation. The enhancement of SF causes the increase of intrinsic wettability, equally amplifying the wettability towards both water and oil (**Figure 3**).[4,39] There are three-type models to describe the effect of surface roughness on wettability. In the first situation, the wettability is regarded to be only affected by the liquid–solid contact region. On this occasion, the surface is completely wetted by the liquid, and Wenzel's model[72] is adopted as follows:

$$\cos\theta^* = R_f \cdot \cos\theta_Y \quad (2)$$

Where θ^*, R_f represent the apparent contact angle and surface roughness, respectively. From this Equation, it can be clearly noticed that the $\cos\theta^*$ is linearly correlated to the R_f. Since the R_f is defined as the ratio of actual surface area to the geometric projected area, the improvement of contact angle can be interpreted as the enlarged contact area between water and hydrophobic solid surface. Note that in this situation, the water droplet completely wet the rough surface, hence the water repellency is in proportion to the surface roughness. However, sometimes the $\cos\theta^*$ from experiments deviated from the linear relationship in Equation (2), especially at very high contact angle region. This can be attributed to the trapped air pocket in the highly rough surface, which means that the hydrophobicity is contributed by the combination of solid surfaces and air, thus leading to the breakdown of the Wenzel's model. It should be noted that herein the water droplet sits on this "mixed" surface without any penetrating. On this occasion, the apparent contact angle can be expressed by Cassie and Baxter Equation[73] as follows:

$$\cos\theta^* = f_1 \cdot \cos\theta_Y + f_2 \cdot \cos\theta_a \quad (3)$$

Where the f_1 represent the fraction of projected area of the surface wetted by the solid surface, and f_2 represent the fraction of liquid-air contact area. Then we have $f_2 = 1 - f_1$ θ_a represent the contact angle of water on air, which is always regarded as 180°. Hence, the Equation (3) can be further converted to follows:

$$\cos\theta^* = f_1 \cdot (\cos\theta_Y + 1) - 1 \quad (4)$$

However, in most cases, the wetting state is the combination of Wenzel and Cassie state, which means the water droplet partially wet the rough surface. In this situation, the water can experience partial surface roughness of the solid surface. Hence, the Equation for this mixed state can be derived from Equation (3) as follows:

$$\cos\theta^* = f_1 \cdot R_f' \cdot \cos\theta_Y + f_2 \cdot \cos\theta_a \quad (5)$$

Where the R_f' represents the surface roughness of wetted solid surface, i.e., the part that experienced by the water droplet ($R_f' < R_f$). Correspondingly, the Equation (4) can be converted to following form:

$$\cos\theta^* = f_1 \cdot \left(R_f' \cdot \cos\theta_Y + 1\right) - 1 \quad (6)$$

It is known that flat surface can only achieve limited wettability (e.g., moderate hydrophobicity, contact angle less than 120°) even with extremely low surface energy coatings.[70,71] Additionally, from the fundamental mechanism analyzed above, enhanced surface roughness can not only significantly increase/decrease the apparent contact angle, but also amplify the difference of oil/water wettability.[4,39] Thereby, the development of highly rough solid surfaces by devising well-defined microstructures have drawn dramatic attentions.

The appropriate surface wettability is extremely important for water remediation. For oil/water separation, the high water/oil selectivity is the only requirement, hence either hydrophobic/oleophilic or hydrophilic/under water oleophobic materials can be used. For selective oil uptake, hydrophobic/oleophilic materials are always employed to achieve high efficiency and large adsorption capacity. However, as shown in the **section 2.1**, a

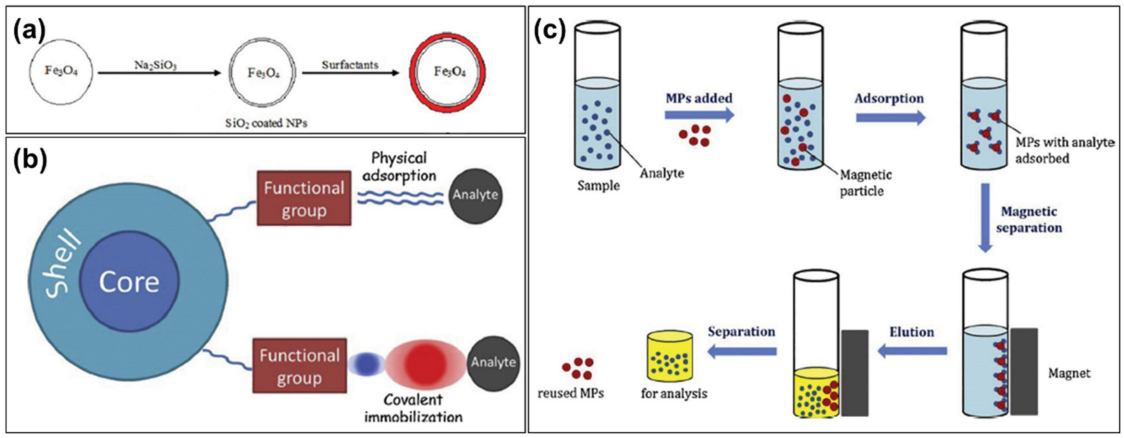

Figure 4. a) Typical synthetic routes of magnetic powders (MPs). Reproduced with permission.[74] Copyright 2014, Wiley-VCH. b) The typical structure of commonly prepared MPs. Reproduced with permission.[27] Copyright 2013, Elsevier. c) The procedure of using MPs for magnetic solid phase extraction (MSPE). Reproduced with permission.[27] Copyright 2013, Elsevier.

certain degree of hydrophilicity at external surfaces is beneficial for treatment of submerged oils. For the removal of heavy-metal ions and dyes in water, hydrophilic materials with appropriate active sites are required. Hence, the required wettability of materials is on account of application fields.

2.3. MPs and 3D-SPMAs

Since the magnetic powders have been utilized in water remediation for a long time, it is essential to carefully compare the features of MPs and 3D-SPMAs, so as to learn from experiences of MPs and find the unique features of 3D-SPMAs for their better use.

Magnetic powders are always magnetic particles with the size from nanometer-level to micrometer-level. These small-size magnetic particles are always engineered to a surface-modified core–shell structure, which is beneficial to combine advantages of large specific surface area, large number of surface active sites, and no secondary pollutants.[27] Based on this configuration, the synthesis process typically involve three steps, i.e., the synthesis of magnetic cores, coating the magnetic cores, and the modification of the core–shell structure (**Figure 4**a,b).[27,74] MPs have been widely used in adsorption/enrichment of heavy-metal ions and dyes in water for water remediation or pollutants detection (Figure 4c). The corresponding adsorption mechanism can be either chemical adsorption (e.g., redox reactions) or physical adsorption (e.g., electrostatic interactions), depending on the surface properties of MPs and adsorbates.[32] After adsorption, MPs are separated from the system by an external magnetic field and regenerated by desorption with appropriate solvents. To release the particles after use, superparamagnetism powders that do not have "magnetic memory" are preferred.[29,74] On the other hand, MPs have also been investigated for oil spill removal in water.[75–78] For example, Zhu et al.[76] prepared hydrophobic core–shell Fe_2O_3@C nanoparticles for selective on-water oil adsorption. Considering the treatment of submerged oil, Abbaspourrad et al.[77] devised unique hydrophobic porous core/hydrophilic shell structures functionalized by iron oxide nanoparticles. The resultant materials can adsorb considerable amount of organic molecules (decane hydrocarbon oil) while remaining well dispersed in water.

However, there are some unavoidable challenges when MPs are applied in practical applications. First, the small-size particles are easy to aggregate during preparation and recycling process.[27] Although the appropriate surface coating and modification can mitigate the aggregation to some extent, it is always at the cost of degraded performance (e.g., adsorption capacity, magnetism). Second, based on the operation principle, theoretically only superparamagnetic powders are allowed,[29,74] more or less limiting the available materials or synthetic methods. Third, although MPs can be theoretically retrieved after usage, it is not easy in reality to completely collect these small-size matters especially when they are used in a large-scale condition.[33,34,79] Finally, the oil uptake capacity of MPs is typically less than 10 times weight gain, far lower to meet requirements for practical applications. This is due to the adsorbed oil can only be accommodated in the volume of particles themselves (**Figure 5**a).

3D self-supporting porous magnetic assemblies, on the other hand, are capable of addressing nearly all issues faced by MPs mentioned above. 3D-SPMAs are macroscopic, free-standing 3D crosslinked networks that contain quasi-uniformly distributed magnetic components. Base on this configuration, magnetic components are naturally and permanently dispersed in networks without aggregation even during repeated use, ensuring large specific surface area and sustainable high performance. For removal of heavy-metal ions and dyes, the mechanism of 3D-SPMAs is similar to that of MPs, both of which relies on the interactions of adsorbate and adsorbents at the interface. Hence, the processing capacity is mainly determined by the specific surface areas, leading to similar performance of two type materials. Actually, sometimes the 3D-SPMAs are deliberately grinding into powders before using, so as to enhancing the mass transfer. In contrast, for oil uptake, the 3D-SPMAs are directly used without any treatment. The adsorption capacity of 3D-SPMAs is well above that of MPs by the factor of 10 to 100 times, which is attributed to the different adsorption mechanism. For 3D-SPMAs, the adsorbed oil is mainly accommodated in the pores formed by 3D networks (characterized by the porosity, which is typically

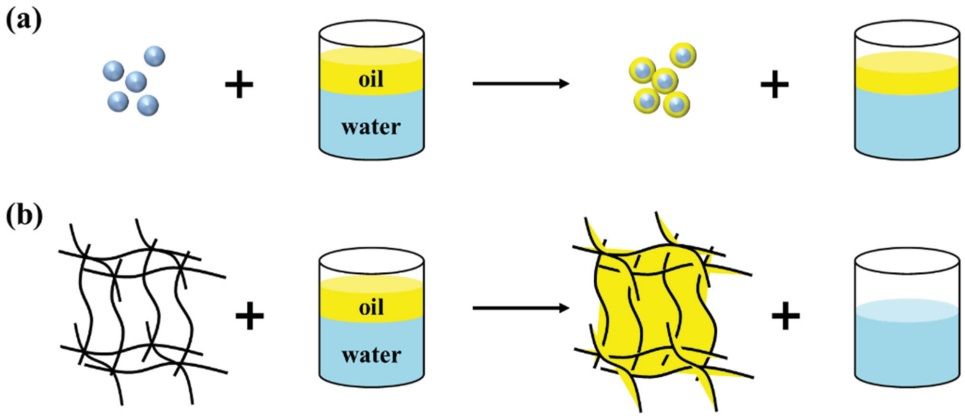

Figure 5. Schematic demonstration of the oil uptake mechanism by using (a) MPs and (b) 3D-SPMAs.

>90 vol.%), the room of which is of several magnitude larger than the solid networks themselves (Figure 5b).

3. Classification and Corresponding Synthetic Strategies of 3D-SPMAs

3D-SPMAs can be either "dry materials" (e.g., aerogels, sponges, foams, whose term are determined according to their preparation methods or common practice) or "wet materials" (e.g., hydrogels). The dry 3D-SPMAs can be further classified in two types, i.e., 3D-SPMAs based on magnetic building blocks and 3D-SPMAs based on magnetic/nonmagnetic mixture (**Figure 6**). Because the methods of acquiring wet 3D-SPMAs are similar to that of dry 3D-SPMAs and certain research works of magnetic hydrogels have been reviewed previously,[54] so 3D-SPMAs based on magnetic hydrogels were only briefly introduced. Based on the above classification, corresponding synthetic strategies are reviewed and in-depth discussed in this section.

3.1. Dry 3D-SPMAs

Dry 3D-SPMAs are herein categorized into two groups, i.e., 3D-SPMAs based on magnetic building blocks (3D-SPMAs-MB) and 3D-SPMAs based on magnetic/nonmagnetic mixture. 3D-SPMAs in the first group often show magnificent magnetic properties due to their complete magnetic compositions. 3D-SPMAs in the latter group, on the other hand, are easy to be tuned to attain desirable structures and functions incurred by the intentionally introduction of other components.

3.1.1. Dry 3D-SPMAs Based on Magnetic Building Blocks

The magnetic building blocks based 3D-SPMAs (3D-SPMAs-MB) are constructed mainly or even entirely by magnetic materials, thus often showing pronounced magnetic properties. In this part, the synthetic methods of 3D-SPMAs-MB including conventional metal foams, nanoporous metal foams/aerogels, and other newly developed materials in last few years

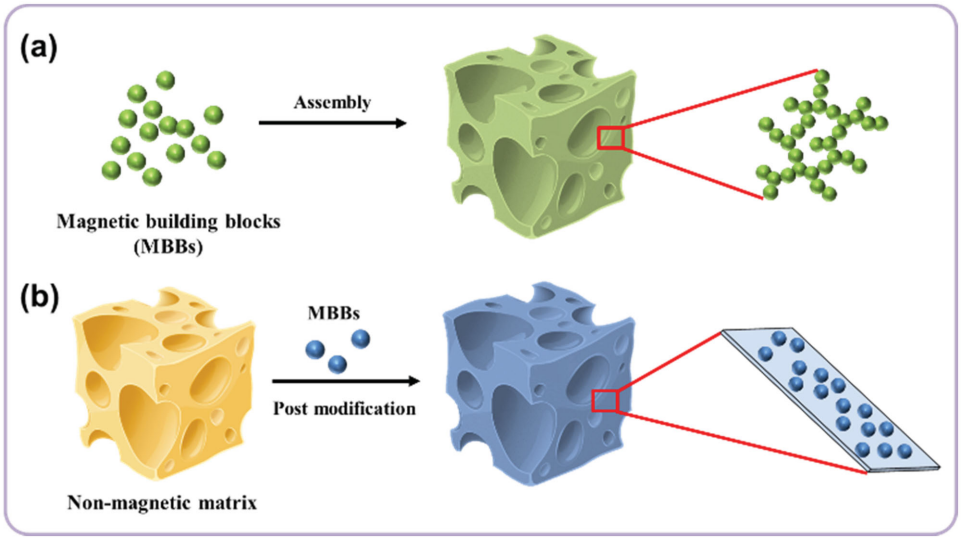

Figure 6. Schematic demonstration of two main types of 3D-SPMAs. The 3D-SPMAsconsist of (a) entirely magnetic building blocks, or (b) magnetic/nonmagnetic mixtures.

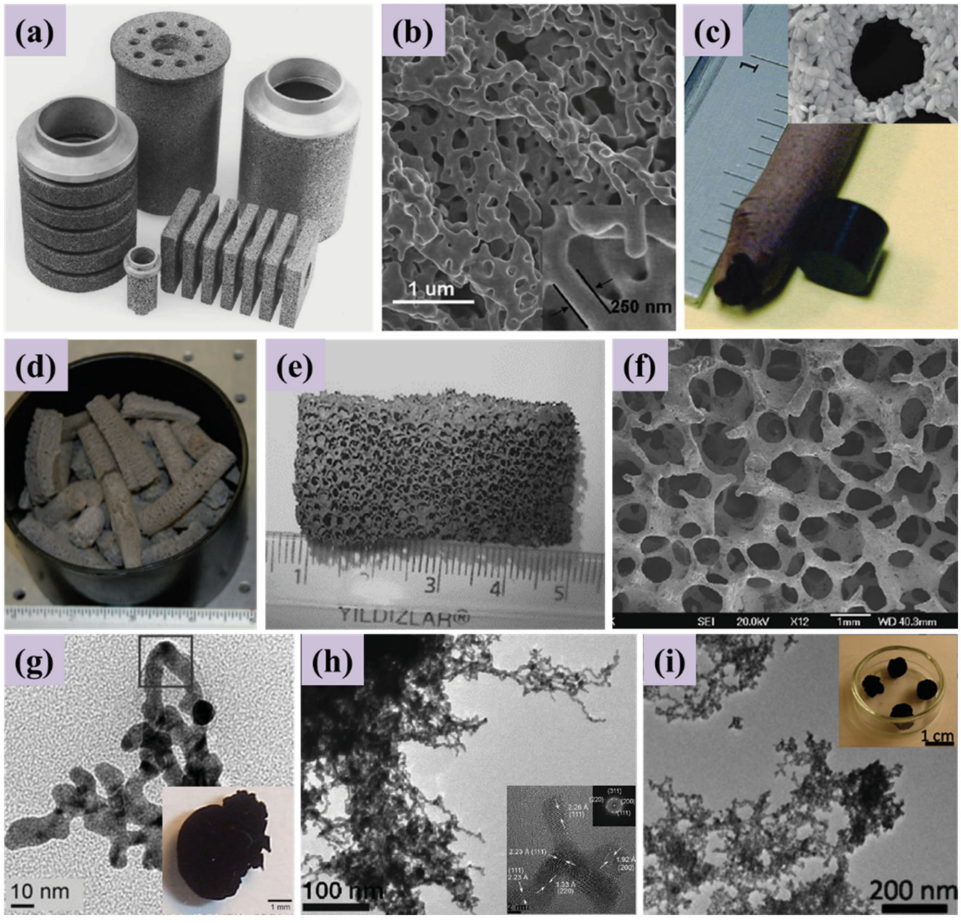

Figure 7. a) Cellular aluminum material made by using space-holding fillers. Reproduced with permission.[81] Copyright 2001, Elsevier. b) SEM images of open-cell Ni foams. Reproduced with permission.[82] Copyright 2012, Royal Society of Chemistry. c) Photograph of iron nanofoam next to an unburned pellet of the Fe-BTA complex. Reproduced with permission.[85] Copyright 2006, American Chemical Society. d) Cobalt nanofoams. Reproduced with permission.[83] Copyright 2010, Wiley-VCH. e,f) Photography and SEM image of a permanently magnetic $BaFe_{12}O_{19}$ foam. Reproduced with permission.[59] Copyright 2010, Elsevier. g–i) TEM images and digital photos of gold/silver hydrogels, $Pt_{50}Pd_{50}$ aerogels, and Pd aerogels, respectively. g) Reproduced with permission.[86] Copyright 2011, Wiley-VCH; h) Reproduced with permission.[88] Copyright 2013, Wiley-VCH; i) Reproduced with permission.[89] Copyright 2014, American Chemical Society.

are introduced in turn. To construct these materials, main approaches include bottom-up assembly of magnetic building blocks (by CVD or sol–gel chemistry following with special drying) and templating methods.

Metal Foams: Metal foams are man-made cellular materials composed by metals and alloys. To distinguish them from nanoporous metal foams/aerogels which will be described in the next part, materials discussed here are referred to conventional metal foams possessing high density and large average pore size. As a kind of long-existing engineering materials, metal foams have been systematically studied and corresponding preparation methods have been summarized previously (**Figure 7**a,b).[80–82] In general, the synthetic methods are divided into three classes, i.e., solid-state processing (SSP), liquid-state processing (LSP), and deposition processes.

The main ideas for SSP and LSP are similar, only difference lies in the phase state of metal precursors. To manufacture metal foams, gas template could be used, where the metal (either liquid metal, metal slurries, or metal powders) is foamed by either directly injecting gas or in-situ generating gas by blowing agents, followed by cooling, compacting or sintering to fix the porous structure. Another route utilizes solid substances as "space-holding materials". Here the metal is mixed with space-holder materials at first, then the holders are removed after the mixture is shaped by drying or compacting, thus producing cellular foams. For deposition strategy, it can be further classified into electro-deposition and vapor-deposition. In the former approach, the metal is electrically deposited on pre-modified polymer foams by reduction of metallic ions from electrolyte. In the later approach, the metal is deposited on the porous substrate from gaseous metal or metal compounds at elevated temperature. After deposition, the template could be easily removed by thermal or chemical treatment and thereby creating metal foams with hollow struts.

It should be noted that although the metal foams have been developed for a long time, most metal foams have not been applied in water remediation. One reason is that their large densities (typically >300 mg cm^{-3}) will significantly reduce the mass-based specific processing capacity. Even so, many methods presented here, such as gas/solid templating,

electro-deposition, and vapor deposition are inspiring for preparing other 3D-SPMAs.

Nanoporous Metal Foams/Aerogels: Nanoporous metal foams/aerogels (NMFAs) are a kind of emerging 3D metal-based materials, which is defined as metal-based 3D structures exhibiting a porosity of above 50%.[83] They often show much lower density and higher specific surface area than conventional metal foams discussed above. Combining high conductivity and catalytic activities, NMFAs have drawn dramatic interests since its appearance. NMFAs based on gold, silver, platinum, palladium, copper, and some magnetic metals (iron, cobalt, and nickel) have been fabricated in last few years (Figure 7c,d), which provides great opportunities in producing unique materials for a wealth of applications.

Main approaches of NMFAs preparation consist of nanomelting, templating, combustion synthesis, and sol–gel assembly.[83–89] For example, free-standing nickel films with ordered, monodispersed pores have been synthesized by electroless deposition templating silica spheres.[84] Nanoporous metal foams can also be produced by nanomelting technique.[90] In detail, the resorcinol–formaldehyde (RF)/metal oxides hybrid aerogels are pyrolyzed in inert atmosphere, during which process RF evolves into carbon and carbon oxides (e.g., CO, CO_2), in situ reducing the metal oxides to metallic elementary substances. In another work, ultralow-density nanostructured metal foams have been derived from combustion of transition-metal complexes containing high nitrogen energetic ligands, such as the metal complexes of energetic ligand bistetrazolamine (BTA) under inert environments.[85] During this course, the complexes showed a steady burning behavior, ensuring the monolithic architecture of products. Additionally, the high-nitrogen ratio provides both heat for decomposition and gas for foaming, and the presence hydrogen from ligand provides a reducing environment for stabilizing metal atoms at zero-valence state. A variety of noble metal aerogels based on Au, Ag, Pd, Pt have also been created by sol–gel chemistry followed by supercritical drying (Figure 7g–i),[86,88,89] where the photo, oxidants, alcohols, or multi-valence anions were used to controlled destabilize the sol of metal nanoparticles and thus inducing gelation.

These NMFAs combining small-size pores, different magnetic properties, and all-metal backbones may exhibit certain novel properties different from traditional macrocellular metal foams and other 3D-SPMAs. However, until now few works have investigated the magnetic-related properties and applications of these NMFAs. Additionally, no work mentioned the applications of them on water remediation, probably due to their weak mechanical strength or relatively higher density compared with other 3D-SPMAs based on, e.g., polymers and carbon materials.

Other Materials: In last few years, several types of new 3D-SPMAs-MB with distinct features from above metal foams have been developed, showing great promise in water remediation.[35,38,41,58,59,91–93]

For example, Brown et al. prepared low-density Fe_2ZnO_4 aerogels (≈12–15 mg cm^{-3}) by epoxide-induced co-precipitation of ferric nitrate and zinc nitrate followed by supercritical drying.[58] For some metal salts with low solubility, templating can be an alternative choice. Topal et al.[59,91] fabricated permanently magnetic $BaFe_{12}O_{19}$ foams by loading polyurethane foam with the precursor slurry containing insoluble metal salts, followed by pyrolysis and sintering. The as-obtained $BaFe_{12}O_{19}$ foam showed saturation magnetization (Ms) of 56.5 emu g^{-1}, remanence magnetization (M_r) of 12.1 emu g^{-1}, and coercive fields (H_c) of 580 Oe. Similarly, Ni–Mn–Ga foam was produced by replication method by using hierarchical-sized sodium aluminate powders as the template.[35] It can be seen that all above examples more or less borrowed methods from metal foams or NMFAs.

Recently, to acquire low-density 3D-SPMAs with suitable mechanical properties for oil adsorption, Chen et al.[38] produced ultralight and mechanically robust magnetic Fe_2O_3/C, Co/C, and Ni/C foams with density <5 mg cm^{-3} (**Figure 8**a). The foams were derived by grafting metal acrylate on PU foams mediated by polyacrylic acid (PAA) modification and ion exchange at first, followed by pyrolysis to remove the PU foams and develop magnetic materials. In another work, Kong et al.[93] reported the scalable synthesis of three-dimensional mesoporous iron oxide (3DMI) also by using PU foam as the template. As shown in Figure 8b, in this work, Prussian blue (PB) was used as the porous coordination polymer network (PCPN), which was grown on PU foams with a mesoporous nano-cube architecture. Then the PB nano-cube loaded PU foam was converted to 3DMI by pyrolysis, where a 3D macroporous network constructed by mesoporous nano-cubes was obtained. Thanks to this hierarchical macro- and mesoporous structure, 3DMI exhibited ultralow density (6–11 mg cm^{-3}) and large specific surface area (ca. 117 m^2 g^{-1}). It also possess a high M_s of 40–60 emu g^{-1}.

For all examples shown above, magnetic materials are directly exposed to the external environment, which may lose the magnetism under certain circumstances. To address this concern, magnetic CNT (Me-CNT) sponges were developed (Figure 8c–e). Gui et al.[41] found that the introduction of high concentration of ferrocene during chemical vapor deposition (CVD) can lead to magnetic CNTs filled by iron nanowires, which means the magnetic iron is protected by the inert and solid CNTs shells. Thus, Me-CNT showed not only a relatively high M_s of 21.1 emu g^{-1}, but also extraordinary cycling performance for oil adsorption.

3.1.2. Dry 3D-SPMAs Based on Magnetic/Nonmagnetic Mixtures

The 3D-SPMAs based on solely magnetic building blocks often possess high magnetism, whilst the introduction of nonmagnetic building blocks can be beneficial to enhance certain physical properties, improve the controllability of the morphology, and impart new functions in materials. In this part, the synthetic strategies are introduced based on two categories, i.e., in-situ preparation and post modification methods.

In Situ Preparation: In this class, 3D-SPMAs are obtained by one step, largely simplifying the procedures and saving the production time. Fe_3O_4 powders are frequently incorporated in the 3D assemblies by in-situ molding,[94] sol–gel transition,[42,95–97] lyophilization,[43] or electrospinning,[98] so as to acquire magnetic bulk materials. For instance, Ge et al.[94] produced superhydrophobic materials by directly

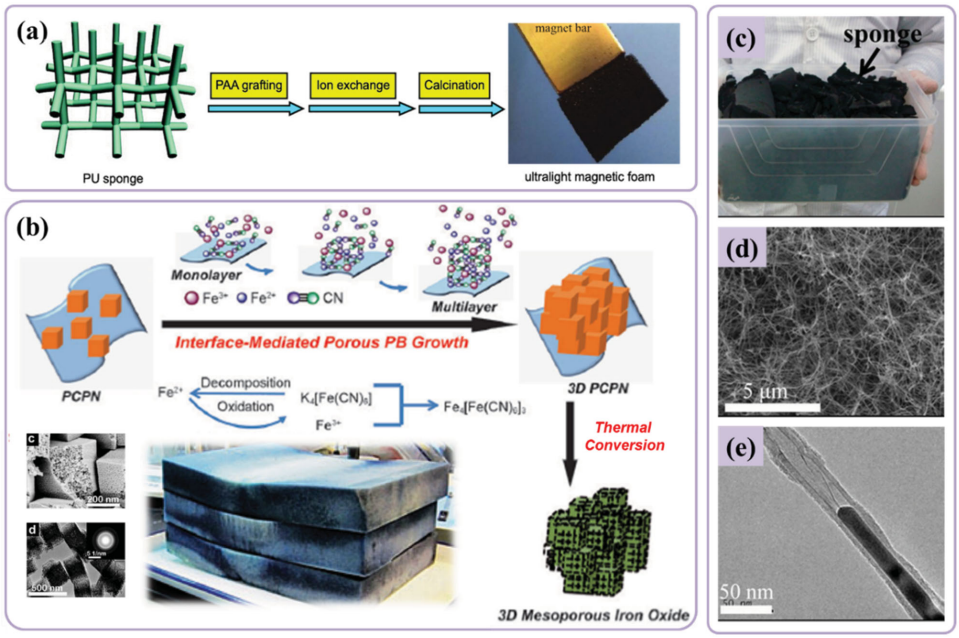

Figure 8. a) Magnetic metal/carbon aerogels derived from polyelectrolyte–grafted polyurethane (PU) foams. Reproduced with permission.[38] Copyright 2013, American Chemical Society. b) Three-dimensional mesoporous iron oxide (3DMI) architectures acquired from interface-induced growth and self-assembly on 3D frameworks and following pyrolysis step. Reproduced with permission.[93] Copyright 2014, Wiley-VCH. c–e) Magnetic CNTs sponges derived from CVD growth. Reproduced with permission.[41] Copyright 2013, American Chemical Society.

mixing CNTs, polytetrafluoroethylene (PTFE), and Fe_3O_4 powders in water/chloroform solution together, followed by drying and hot-pressing to hold the monolithic shape. However, it is not surprising to obtain a high-density and low-porosity material by using this approach. To improve the stability of magnetic materials (e.g., γ-Fe_2O_3) or mechanical performance of whole materials, silica or silicone has been utilized as the continuous networks, and usually magnetic core/SiO_2 shell nanoparticles were in-situ incorporated in the 3D networks during the gelation of silicone.[44,99–101] The resultant materials showed typically magnetism ranging from 10 to 30 emu g^{-1}. For example, Li et al.[101] fabricated porous silicone sponges polymerization of organo-silanes in the presence of Fe_3O_4@silica nanoparticles (**Figure 9**a), which featured fast magnetic responsivity, superhydrophobicity/superoleophilicity, high compressibility and stability. Another study showed the preparation of the $CoFe_2O_4$-SiO_2 and $NiFe_2O_4$-SiO_2 aerogel nano-composites by calcinating urea-assisted prepared silica aerogels containing iron and cobalt or iron and nickel, showing M_s less than 10 emu g^{-1} at 5 K.[100]

Recently, researchers noticed more functions of magnetic materials or its precursors apart from simple magnetism integration.[45,62,102,103] Thanikaivelan et al.[102] and Li et al.[45] have used the surface-modified magnetic particles to stabilize the components accounting for networks formation. In another study, Chen and co-workers[103] obtained graphene/γ-Fe_2O_3 aerogels by in-situ hydrolysis of $FeCl_3$ in the presence of GO followed by drying and calcination (Figure 9b). The gelation might be the synergistic effect of electrostatic interactions between positively-charged Fe(III) ions or $Fe(OH)_3$ colloidal particles and negative-charged GO sheets, as well as the aggregation of $Fe(OH)_3$ colloidal particles and GO sheets. The M_s of aerogels ranges from 23 to 54 emu g^{-1}, depending on the content of γ-Fe_2O_3. Interestingly, the hybrid aerogel is composed by two separate networks of graphene and Fe_2O_3, respectively. Hence, it can be transformed to the free-standing, solely γ-Fe_2O_3 aerogel by simply calcination in air. In a recent work, Cong et al.[62] subtly used iron(II) ions to reduce graphene oxide and simultaneously deposit magnetic Fe_3O_4 nanoparticles during gelation, thus producing ferromagnetic aerogels with M_s up to 80.3 emu g^{-1} (Figure 9c).

Taking advantage of responsive properties of magnetic components towards external magnetic field, the in-field preparation of magnetic aerogels for anisotropically-structured materials have also been studied.[36,37] Gich et al.[36] fabricated magnetic silica composite aerogels (Figure 9d) by conducting reaction in an 8000 Oe homogeneous magnetic field. The magnetic $Nd_2Fe_{14}B$ particles showed a needle-like arrangement in the gel, which is induced by the alignment of magnetic particles along the direction of magnetic field during the gelation of silica. This unique anisotropic structure endowed aerogels with quite different optical properties compared with homogeneous gels. Heiligtag et al.[37] produced a series of anisotropically structured anatase–magnetite composite aerogels (Figure 9e) by either mold-assisted stepwise gelation or magnetic-field assisted in-field gelation. The methods are capable of producing diverse anisotropic magnetic texture which might be useful in photocatalysis.

Postmodification: 3D-SPMAs based on magnetic/nonmagnetic mixture are often composed of 3D nonmagnetic networks and integrated magnetic components. The distinct advantage of this method is the decoupling of the construction of 3D networks and magnetism integration, which allows much more flexible materials engineering. In this manner, it is favorable to separately or stepwise process the nonmagnetic and the

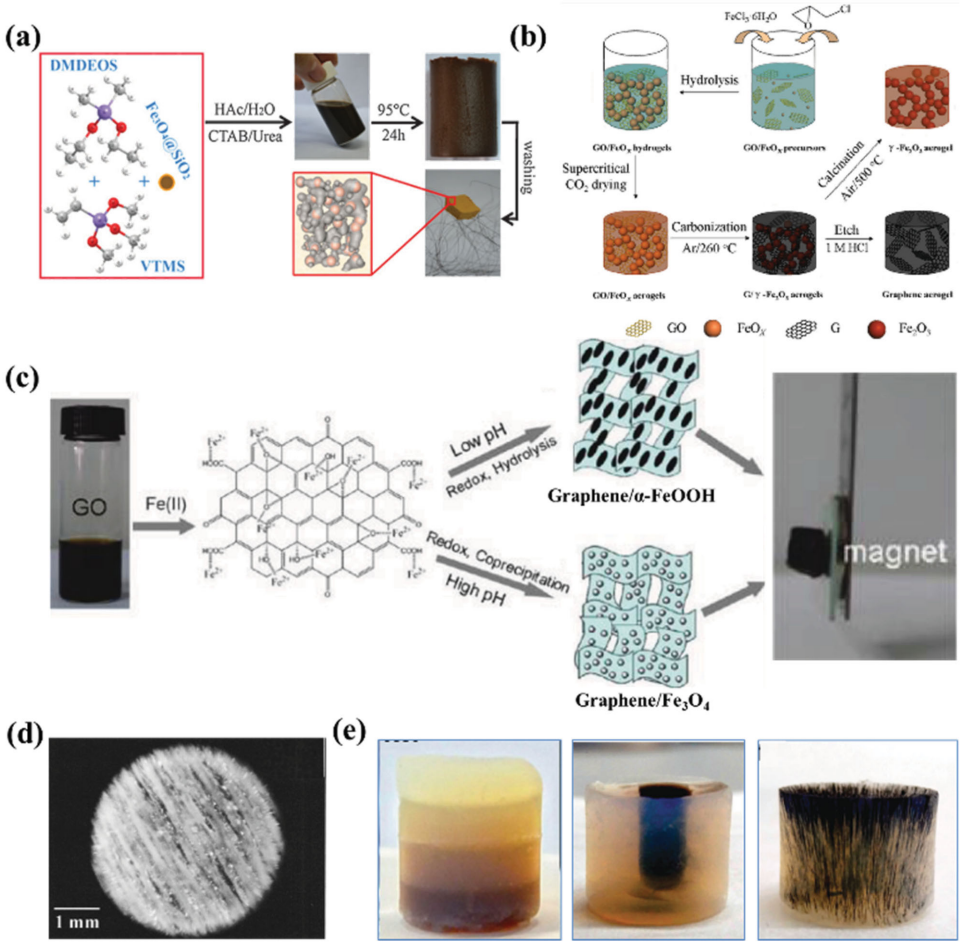

Figure 9. a) Silicone sponges derived from polymerization of organo-silanes in the presence of Fe_3O_4@silica nanoparticles. Reproduced with permission.[101] Copyright 2014, Royal Society of Chemistry. b) Synthetic route of graphene/γ-Fe_2O_3 hybrid aerogels with double nano-crystalline networks. Reproduced with permission.[103] Copyright 2013, Wiley-VCH. c) Preparation of graphene-based aerogels by a metal ion induced self-assembly process. Reproduced with permission.[62] Copyright 2012, American Chemical Society. d) The photograph of silica/$Nd_2Fe_{14}B$ particles composite aerogel synthesized in the presence of 8 kOe homogeneous magnetic field. Reproduced with permission.[36] Copyright 2003, American Institute of Physics. e) A variety of anisotropic anatase–magnetite aerogel monoliths obtained by either stepwise gelation (left), templating (middle), or in-field gelation (right) process. Reproduced with permission.[37] Copyright 2014, Royal Society of Chemistry.

magnetic part, which facilitates expanding the available materials for 3D-SPMA preparation. Additionally, in this way, the structures or properties of materials can be precisely controlled and optimized, which is beneficial for intentional design and promotion of the overall performance. Moreover, many commercial and low-cost sponges and foams can be used as the 3D networks, significantly reducing the production cost and simplifying the synthetic procedures. In this section, because the employed 3D networks are readily available commercially or experimentally, hence the emphasis is often placed on post modification of as-obtained 3D networks.

Many works separately prepared magnetic precursors' dispersion and other components (e.g., solution of fluoro-alkyl silane (FAS) for creating low-energy coatings on materials) before modifying as-obtained 3D networks.[33,34,104–107] For example, Calcagnile et al.[33] produced magnetically driven floating foams by decorating as-prepared spinel-cubic γ-Fe_2O_3/Fe_3O_4 nanoparticles on PU foams, followed by PDMS deposition by triboelectric charging (**Figure 10**a). The spinel-cubic γ-Fe_2O_3/Fe_3O_4 nanoparticles provided high surface roughness and PDMS offered intrinsic hydrophobicity, thus generating highly hydrophobic materials. In another interesting work, Yang et al.[107] described a multifunctional melamine foam (MF) based sponge (UHF sponge) by an extremely simple adsorption-combustion process (Figure 10c–f). In detail, MF adsorbed a certain amount of organic solvent (e.g., toluene) before burning in air, after which the surface of MF was loaded with hydrophobic amorphous carbon microstructures, thus producing hydrophobic MF. The magnetism can be facilely integrated by replacing the carbon source with toluene suspension of Fe_3O_4 nanoparticles. However, the stability of decorated carbon microstructures should be improved before applying them in practical use.

On the other hand, magnetic materials can also be in-situ fabricated on as-obtained 3D networks.[79,108–113] Olsson et al.[79] have in-situ produced $CoFe_2O_4$ nanoparticles on bacterial cellulose aerogel template by participation of $FeSO_4$/$CoCl_2$ solution in the presence of NaOH/KNO_3. It is well known that the fabrication of microstructures on 3D substrates with high

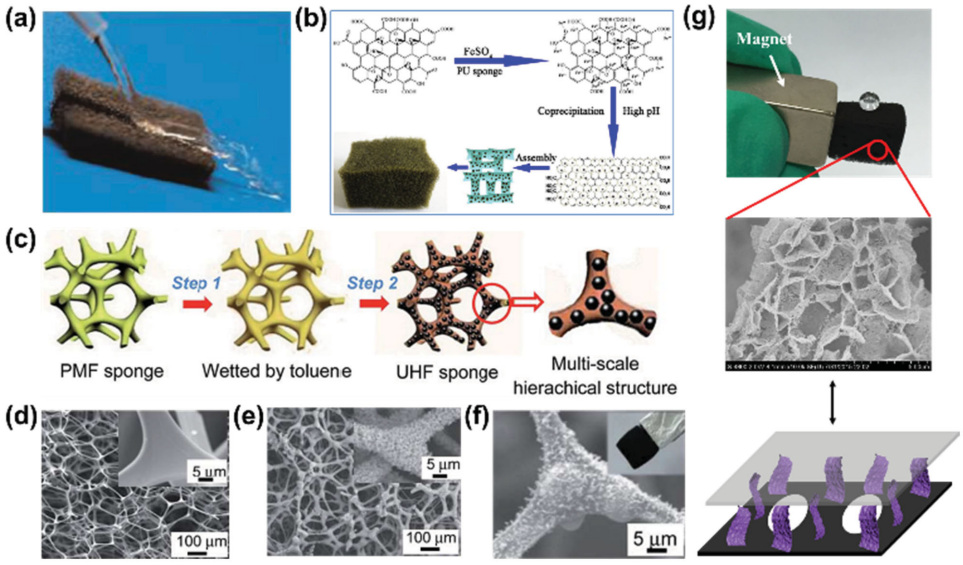

Figure 10. a) Superhydrophobic PU/Fe_xO_y foams derived from post modification of magnetic nanoparticles and PDMS. Reproduced with permission.[33] Copyright 2012, American Chemical Society. b) Preparation of PU/graphene/Fe_xO_y foams by in-situ co-precipitation of graphene oxide and $FeSO_4$. Reproduced with permission.[113] Copyright 2014, Elsevier. c–f) Synthetic strategy and corresponding morphology of melamine-based sponges by an adsorption–combustion method. Reproduced with permission.[107] Copyright 2015, Royal Society of Chemistry. g) Melamine foam based superhydrophobic and magnetic 3D materials with 0D/2D hybrid-dimensional microstructures. Reproduced with permission.[39] Copyright 2016, Royal Society of Chemistry.

roughness and well-defined structures is important to obtain superwettable bulk materials with predictable wettability. Recently, we have extracted the dependence between the wettability and the dimensions of microstructures on melamine foams.[4] The result showed that hybrid dimensions can significantly enhance the wettability by a multiply rule. On this basis, by further manipulating the chemical composition, we have created unique magnetic cobalt based microstructures with hybrid dimensions, i.e., zero dimensional (0D) nano-size particles composed two-dimensional (2D) microsized sheets on melamine foams by controlled precipitation of cobalt (II) ions followed by reductive annealing (Figure 10g).[39] Herein, the magnetic components provided not only magnetism for remote controllability ($M_s \approx 49$ emu g^{-1}), but also high surface roughness (>6) for amplified wettability. Considering the thermostability of materials, we have utilized highly stable quartz fiber as the 3D substrate to support magnetic structures by similar methods.[40] In this work, the obtained superhydrophobic, magnetic and flexible quartz fiber showed a wide working temperature from –196 to ≈1000 °C, enabling its use in harsh conditions.

3.2. Preparation of Hydrogel-Based 3D-SPMAs

Magnetic hydrogels, as the most important representatives of wet 3D-SPMAs, have also been widely applied in water remediation, especially for removal of metal ions and dyes in aqueous solution. The synthetic methods of them can be divided in two main groups.

In the first group, magnetic materials are loaded on the as-prepared hydrogel matrix.[114,115] For example, Ozay et al.[114] produced magnetic hydrogels by saturating as-obtained dried hydrogels with Fe(II) and Fe(III) ion aqueous solution, followed by transferring the hydrogels into NaOH solution and drying for deposition of magnetic Fe_3O_4 particles (**Figure 11**a).

In the second group, magnetic particles are in-situ enrolled in the 3D networks during the gelation process.[46,47,49,50,116,117] Herein, magnetic particles can serve as either solely magnetic components for magnetism integration, or dual roles for both magnetism integration and crosslinkers promoting gelation. For example, Zhang et al.[46] dispersed carboxy-modified Fe_3O_4 nanoparticles in chitosan solution to form a stable ferrofluid at first, followed by the addition of the telechelic difunctional poly(ethylene glycol) (DF-PEG) to proceed Schiff reaction between chitosan and DF-PEG for crosslinking (Figure 11b). In another work conducted by Messing and co-workers,[118] magnetic cobalt ferrite nanoparticles (NPs) were modified with unsaturated methacrylic groups before subjecting to the reaction solution of acrylamide (AAm) monomer and initiator, where each magnetic NPs could form several covalent bonds with resultant PAAm, thus serving as nanocrosslinkers of the hydrogel's network. In this way, the modulation of magnetic particles could be transferred to the hydrogel's network, thus realizing specific magnetic-related properties. This concept has also been adopted by several following works.[117,119]

4. Applications of 3D-SPMAs in Water Remediation and Beyond

Combining the free-standing 3D architecture, porous structures, tailored magnetism, large specific surface areas, and large processing capacity, 3D-SPMAs have found a wide range of applications, especially in water remediation such as oil uptake, oil/water separation, and removal of dyes or heavy-metal ions

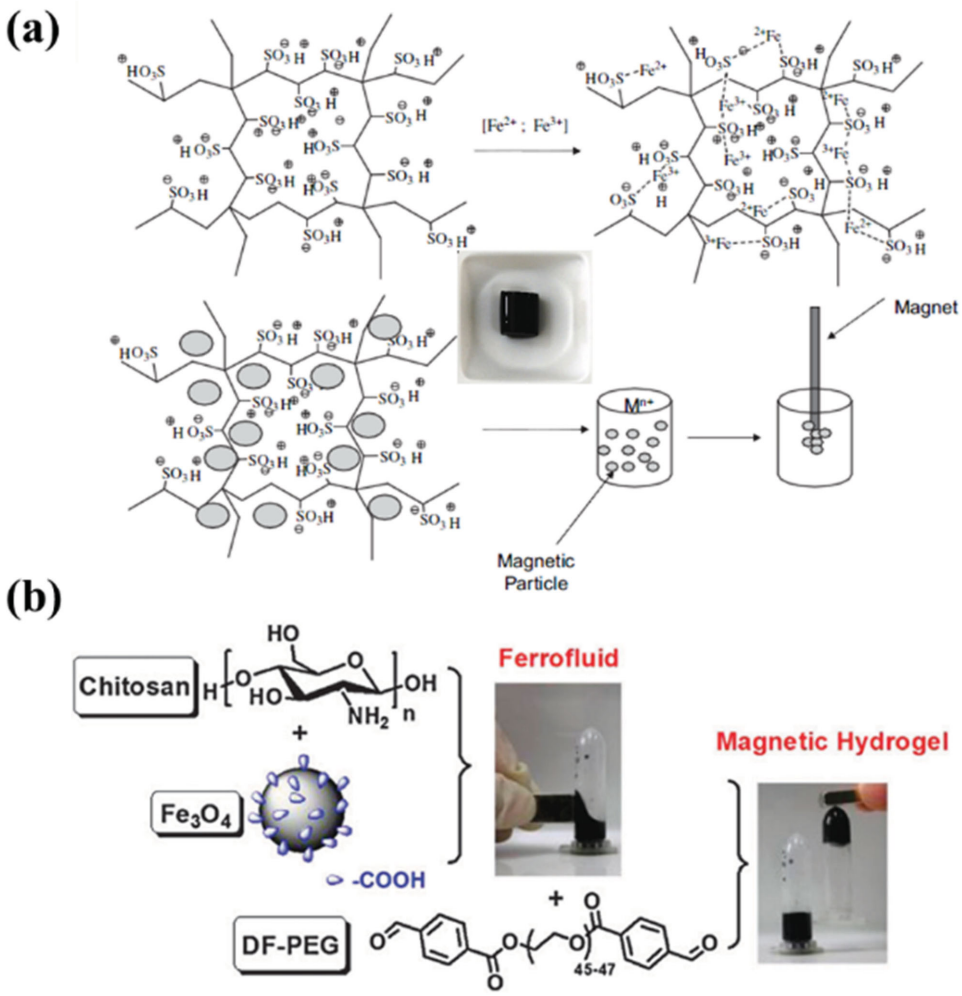

Figure 11. a) Schematic illustration of fabrication of magnetic p(AMPS) hydrogel composite and its application for removing toxic metals. Reproduced with permission.[114] Copyright 2009, Elsevier. b) Synthetic process of chitosan–Fe_3O_4 based magnetic dynamic hydrogel. Reproduced with permission.[46] Copyright 2012, Royal Society of Chemistry.

(**Figure 12**). The magnetic properties and water remediation performance of 3D-SPMAs are summarized in **Table 1**. In this section, the use of "dry" 3D-SPMAs in water remediation and other potential applications are introduced in Section 4.1–4.2. Corresponding applications by using hydrogel-based 3D-SPMAs are discussed in Section 4.3–4.4. Finally in Section 4.5, the pros and cons of using 3D-SPMAs in water remediation are summarized.

4.1. "Dry" 3D-SPMAs for Water Remediation

"Dry" 3D-SPMAs, taking advantage of their empty internal space and high specific surface areas, manifest great practical potential in diverse water remediation applications including oil uptake, oil/water separation, dyes removal, heavy-metal ions elimination, etc.

4.1.1. Oil Uptake

The oil uptake is one of the most flexible and cost-effective methods to remove oil spills from water. Compared with oil/water separation, the direct oil uptake process can process large-scale oil spills pollution without precollection of oil/water mixture. 3D-SPMAs are highly favorable for this application, because they combine the remote controllability originated from the magnetic components, and the high adsorption capacity stemmed from the porous and low-density 3D networks. To maximize the efficiency of oil adsorption in practical oil/water mixture system, the high water repellency is required to enable sole adsorption of oil spills. Based on this consideration, for oil uptake by using 3D-SPMAs, sufficiently high hydrophobicity should be imparted in materials. In this section, the main methods to realize hydrophobicity in 3D-SPMAs, the advantages and the challenges of 3D-SPMAs for oil adsorption are sequentially introduced.

Methods to realize hydrophobicity in 3D-SPMAs: There are two types of method for preparing hydrophobic 3D-SPMAs (3D-HMA). In the first class, 3D-HMA were obtained by the post-modification of as-prepared 3D-SPMAs.[4,15,33,34,38–40,44,93,104,106,113] For example, Li et al.[104] have introduced octadecyl chains on the surface of as-prepared

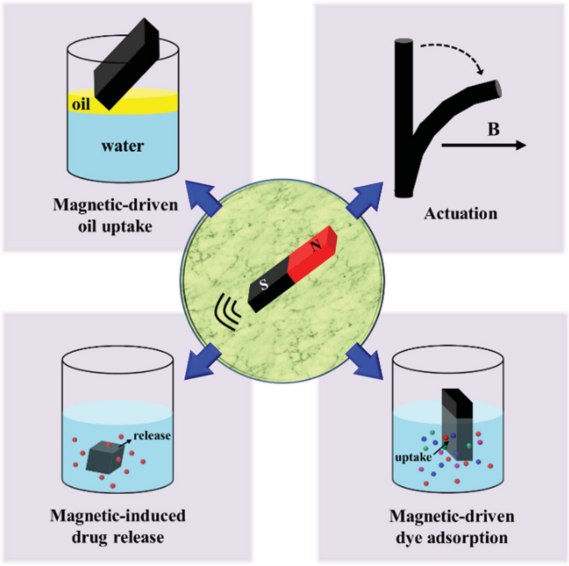

Figure 12. Demonstration of certain representative applications of 3D-SPMAs.

Fe_3O_4-decorated commercial sponges by utilizing the strong interactions between thiol and iron elements. In this way, the whole surface was covered by low-surface-energy alkyl chains, thus acquiring hydrophobicity. Alkyl silane, such as methyltrichlorosilane and octadecyltrichlorosilane have also been used to form a hydrophobic layer on materials' surface by simple dipping-drying process.[34,38,113] In this process, the alkyl silane might hydrolyze and inter-crosslink to form Si–O–Si covalent bonds, thus providing a strong shield to repel water. The silica coating can also account for hydrophobicity. For instance, it can be fabricated by in situ polymerization of tetraethoxysilane (TEOS) via chemical vapor deposition process.[34] To further reduce the surface energy, more hydrophobic materials such as fluoro-alkyl silane (FAS) have also been employed to obtain superhydrophobic 3D-SPMAs.[106]

In the second class, the hydrophobicity was in situ introduced in materials during their preparation.[41,62,94,97,98,101,107] For one case, the hydrophobic additives can be enrolled in the fabrication process.[94,98,107] Yang et al.[107] have developed an extremely facile method to prepared hydrophobic magnetic sponges by simply immersing the pristine sponges in the Fe_3O_4 nanoparticle toluene suspension followed by combustion. During this process, in-situ carbon deposition was realized by the incomplete combustion of toluene which generates rich carbon aggregates covering all surfaces of sponges. The intrinsic hydrophobicity of the carbon and the generated hierarchical microstructures provided the chemical nature of hydrophobicity and the enhanced surface roughness, respectively, thus give rise to highly hydrophobic 3D-SPMAs. For another case, the hydrophobicity was originated from the building blocks themselves.[41,62,97,101] For example, Gui et al.[41] prepared hydrophobic and magnetic CNT sponges by utilizing the intrinsic hydrophobicity of iron-filled magnetic CNTs as building blocks. Li et al.[101] prepared silicon sponges by the polymerization of organosilanes in the presence of silica-coated Fe_3O_4 nanoparticles, thus directly acquiring superhydrophobic materials by taking advantage of hydrophobicity of silanes.

Advantages of 3D-SPMAs in Oil Uptake: The magnetic properties of 3D-SPMAs can greatly facilitate and control the oil adsorption process, thus saving a large amount of human labor. On the one hand, 3D-SPMAs can be remotely driven by a magnet during the adsorption process. In this way, 3D-SPMAs could be easily guided towards the polluted region so as to adsorb floating oil spills. Actually, almost all works about hydrophobic 3D-SPMAs have demonstrated this feature,[4,33,39–41,92,97,106,112] such as CNTs sponges, MWNTs/PDMS nanocomposites, and polyurethane/iron oxide foams (**Figure 13**a-c). However, it should be noted this magnetic-driven adsorption process only accounts for the treatment of on-water oil spills. For underwater oil spills, the magnetic-driven adsorption is always invalidated. Because the attractive force between 3D-SPMAs and the magnet is often insufficient to overcome the repulsion between water and 3D-SPMAs, hence the adsorbents cannot be dragged in the water by the magnet.

On the other hand, after use, 3D-SPMAs can be simply collected by the magnet, avoiding secondary pollution. Several materials, including modified PU sponges and Fe/C nanocomposites have been demonstrated to show this ability (Figure 13d,e).[41,92,106,112] Whereas, it could be foreseen that the 3D-SPMAs can only be collected by the magnetic when they adsorb a small amount of oil. If a large quantity of oil was adsorbed, the 3D-SPMAs would undergo several tens or even several hundred times weight gain. On this occasion, the magnetic attractive force exerted by the magnet may not be able to overcome the gravity of oil-containing 3D-SPMAs, thus failing to collect the as-used adsorbents.

Besides, in contrast with magnetic powders, apart from paramagnetic materials,[34,44,93] ferromagnetic materials[39,41,62] can also be utilized in 3D-SPMAs for oil adsorption. Even if the 3D-SPMAs gained permanent magnetism upon interacting with a magnet, the magnetic components inside 3D-SPMAs would not aggregate because they are fixed by the 3D substrate. Hence, the available materials for fabricating 3D-SPMAs are much wider than that of MPs.

Challenges for Oil Uptake by Using 3D-SPMAs: There are several challenges obstructing the applications of 3D-SPMAs in oil uptake. One challenge is the improvement of the magnetism of 3D-SPMAs. As discussed in the above, the sufficient high magnetism of 3D-SPMAs is desirable for underwater oil adsorption and their collection after use. For the former case, high magnetism is required to overcome the water repellency stemmed from the hydrophobicity of materials and thus allowing 3D-SPMAs to be dragged by a magnet to adsorb submerged oil. For the latter case, high magnetism is desirable to overcome the total gravity of 3D-SPMAs and adsorbed oil, thus enabling collection of as-used 3D-SPMAs by the magnet. Therefore, the selection of integrated magnetic components with high magnetism (e.g., Fe, Co), and maximizing the apparent magnetism of 3D-SPMAs should be considered.

Another challenge is the tradeoff between the adsorption capacity and the magnetism. In most works, the magnetic components are simply enrolled in the materials just accounting for the magnetic integration. In this way, the density of resultant materials increased, which has been proved to be unfavorable

Table 1. Magnetic properties and water remediation ability of some typical 3D-SPMAs.

Material	Saturation Magnetization/emu g^{-1}	Oil Adsorption Capacity/g g^{-1}	Dye or Metal Ions Adsorption Capacity/mg g^{-1}	Ref.
Magnetic CNT sponges	21.1	≈49–56	–	[41]
PDMS/MWNT nanocomposite	–	≈8–21	–	[97]
3DMI	≈40–60	>150	As(III)	[93]
Macroporous Fe/C nanocomposites	–	≈4–8	–	[92]
Fe_2O_3/C foam	≈13 at 1T	≈50–103	–	[38]
Magnetic PU foam	13.4	≈15–72	–	[105]
Magnetic PU foam	–	≈10–35	–	[106]
Magnetic melamine foam	10.8	≈60–160	–	[39]
PU@Fe_3O_4@SiO2@Fluoropolymer Sponges	22.73	≈13–45	–	[34]
PU/iron oxide sponge	–	13.25±1.63	–	[33]
Magnetic carbon fiber aerogel	≈8.8–23.9	≈29–70	–	[112]
Magnetic polymer-based graphene foam	24.1	≈7–23	–	[113]
Magnetic graphene foam	–	≈12–27	–	[111]
CNTs/PTFE/ Fe_3O_4 bulk materials	–	≈0.71–1.15	–	[94]
Magnetic cellulose aerogel	–	28	–	[95]
polystyrene/polyvinylidene fluoride nanofibres	–	≈35–45	–	[98]
Magnetic quartz fiber	12.7	≈50–172	–	[40]
Magnetic silicone sponges	10.0	≈7–17	–	[101]
Magnetic polyester materials	29.89	≈3.5–4.2	–	[44]
Collagen based magnetic nanocomposites	≈0.08	≈1.3–2.1	–	[102]
Graphene/ Fe_3O_4 aerogels	≈45.2–80.3	≈12–27	–	[62]
PS/Fe_3O_4/graphene hybrid aerogel	29.3	≈30–47	–	[42]
Magnetic graphene/Fe_3O_4 sponge	4.4	–	Methylene blue, 526	[43]
Magnetic graphene oxide foam/Fe_3O_4 nanocomposite	40.2	–	Cr(IV) ions, 258.6	[110]
AMPS-based magnetic hydrogels	–	–	Cd(II), Co(II), Fe(II), Pb(II), Ni(II), Cu(II) and Cr(III), ≈76–131	[114]
p(AMPSc-VI)-based magnetic hydrogels	–	–	Metal ions, ≈60–90	[115]
Magnetic cationic hydrogel	≈6	–	Cr(IV) ions, 205	[128]
Magnetic chitosan–Fe(III) hydrogels	–	–	C. I. Acid Red 73, 294.5	[47]

to acquire high adsorption capacity.[15] Actually, the average maximum oil adsorption capacity of those 3D-SPMAs is below 30 times weight gain, which is far lower than normal 3D-SPAs. Although magnetic CNT sponges,[41] carbon fibers based aerogels,[112] and ultralight Fe_2O_3/C foams[38] showed relatively higher capacity of approximately 45 to 60, 30 to 70, and 50 to 103 times weight gain, respectively. They were still insufficient for practical applications.

To address this issue, two routes have been demonstrated. The first one is to reduce the density of 3D materials and thus increasing the pore volume to accommodate oils. Kong et al.[93] fabricated ultralow density (6–11 mg cm^{-3}) 3D magnetic iron oxide frameworks (3DMI) by interfacial assembly of Prussian Blue nanocubes. The resultant hierarchical macro- and mesoporous structures enable their high oil adsorption capacity more than 150 g g^{-1} (Figure 8b, **Figure 14**a). The second method is to improve the wettability of materials towards oils, so as to create a higher driven force to trap oil and fully utilize the existed pore volume. We recently devised a superhydrophobic 3D-SPMAs based on hybrid-dimensional cobalt-based microstructures on melamine foams.[39] Herein, the magnetic cobalt was subtly engineered to form a 0D nanoparticles constructed 2D sheets morphology, which substantially enhanced the wettability of foams (Figure 10g). Together with hydrophobic

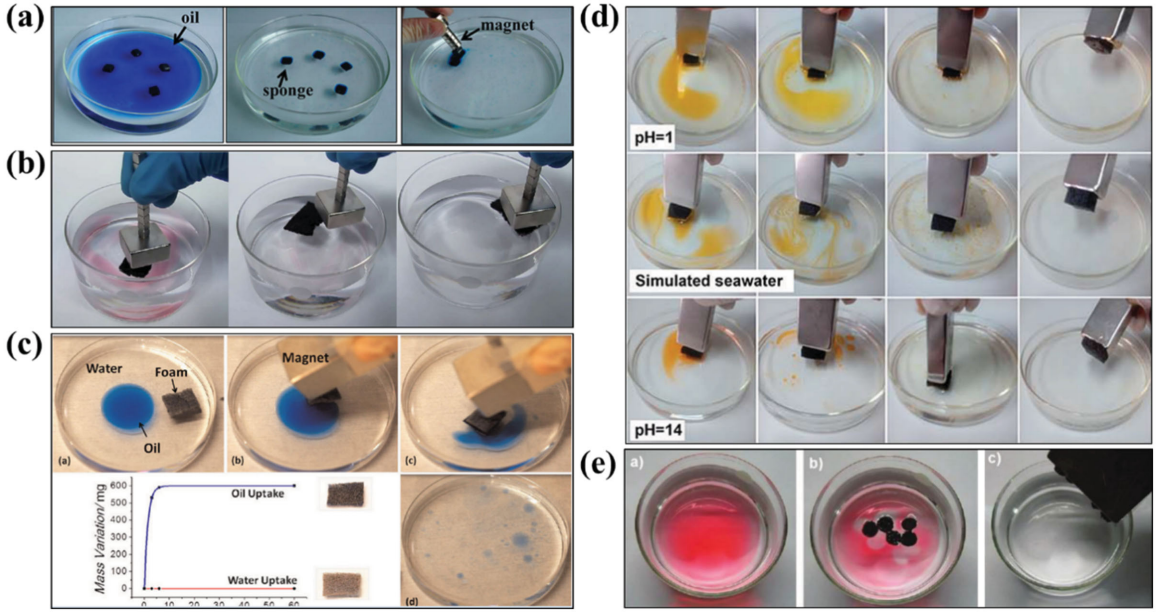

Figure 13. The selective on-water oil uptake with different 3D self-supporting porous magnetic assemblies. a) Magnetic CNTs sponges. Reproduced with permission.[41] Copyright 2013, American Chemical Society. b) Macroporous PDMS/MWNT nanocomposites. Reproduced with permission.[97] Copyright 2015, Royal Society of Chemistry. c) Superhydrophobic PU/Fe_xO_y foams. Reproduced with permission.[33] Copyright 2012, American Chemical Society. d) PU/Fe_3O_4 sponges. Reproduced with permission.[106] Copyright 2015, Royal Society of Chemistry. e) Macroporous Fe/C nanocomposites. Reproduced with permission.[92] Copyright 2012, American Chemical Society.

chemical composition provided by PDMS, the oil spill can be quickly and completely adsorbed driven by large Laplace pressure induced by the high surface roughness. As a result, as shown in Figure 14b, the acquired materials showed not only a high oil adsorption capacity (approximately 60 to 160 times weight gain), but also an ultrafast adsorption behavior (complete adsorption within 1 s). Even though, the further improvement of oil adsorption capacity is still highly desired.

Thirdly, the stability of 3D-SPMAs, including the preservation of the hydrophobicity, the magnetism, and the 3D networks under the certain mechanical force, chemical environment, and temperature, is also the critical problem. Most works focus on the characterization of mechanical stabilities, especially the compressibility of materials. Many 3D-SPMAs showed good compressibility with low plastic deformation (i.e., permanent deformation), indicating good mechanical stabilities. However, it should be noted for practical applications, materials should withstand not only compression deformation, but also shear deformation and tensile deformation. In this regard, it seems that only fibers-based 3D-SPMAs, such as magnetic CNT sponges were qualified. The chemical stability of 3D-SPMAs has also been considered. For example, magnetic CNT sponges showed excellent stability in air, different organic solvents, and aqueous solution with pH values from 1 to 13.[41]

For the thermostability, most works focus on the preservation of 3D networks or the hydrophobicity.[41,93,104,120] For example, both the 3D networks and the superhydrophobicity of CuO-modified textiles were tested under 18–85 °C, showing good stability.[104] Several other materials, including that of CNTs-based, melamine foams based, and Fe_2O_3 nanocubes based 3D-SPMAs can withstand a temperature up to 600 °C in air.[41,93,120] However, at such high temperature, only the preservation of 3D networks was achieved. In fact, the modified magnetic materials and hydrophobic layers are very likely to lose their functions or even decompose at a much lower temperature, e.g., 300 °C. Additionally, the 3D frameworks of most carbon-based materials cannot survive in air at a temperature above 600 °C.[11,12] Imagine that once applied in oil leakage treatment in the sea, most 3D-SPMAs would be completely burned out if the oils were lighted by accidents, thus releasing poisonous gases/ greenhouse gases and causing secondary pollution. In a recent work,[40] we prepared superhydrophobic and ultra-thermostable sponge by using quartz fibers as the substrate to support cobalt magnetic microstructures and hydrophobic PDMS layer. Herein, the quartz fibers are used for the first time to provide both the ultrahigh thermostability of 3D backbones in air (up to 1150 °C) and mechanical flexibility towards a wide range of mechanical forces (Figure 14c,d). We found that although the resultant sponge would lose the hydrophobicity and magnetism at high temperature (>220 °C), it can be readily regenerated by a second round cobalt loading and PDMS deposition even after treatment in air at 1150 °C, which greatly expanded their working temperature ranges. However, the preservation of magnetic properties and hydrophobicity still remain as unsolved challenges.

4.1.2. Oil/Water Separation

As an alternative strategy for water remediation, oil/water separation is much easier to realize automatic operation which is preferred in industrial applications. The main design principle of materials for separation is the high oil/water selectivity. The separation process often happened on the liquid/solid and

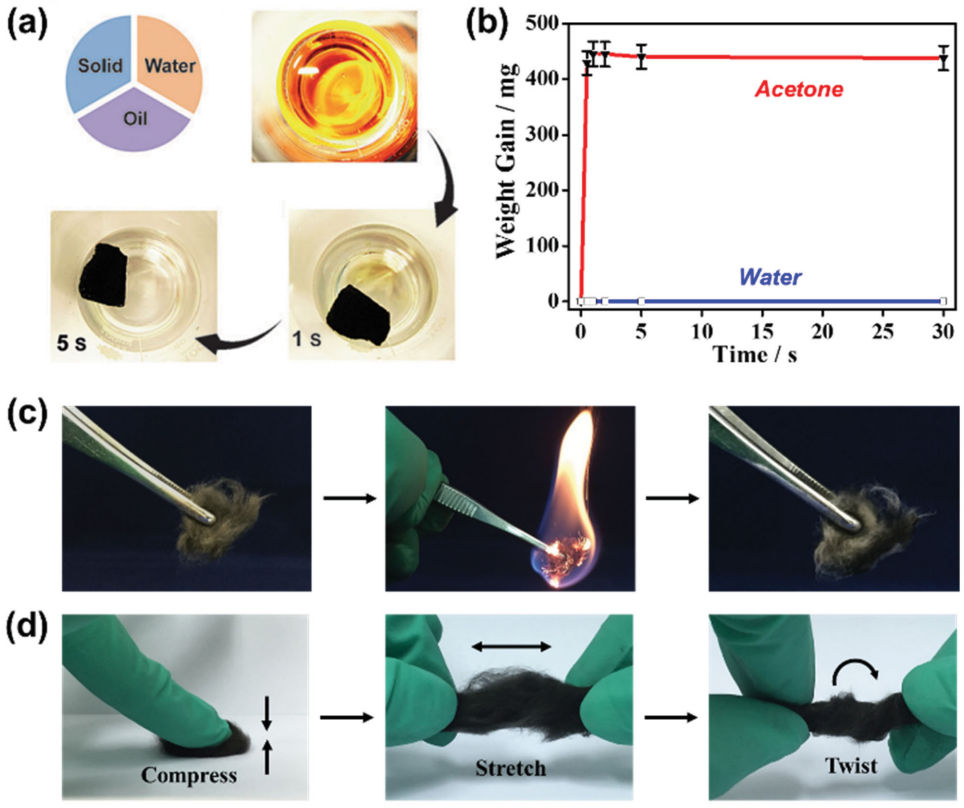

Figure 14. a) Removal of on-water oil by a piece of 3D mesoporous iron oxide aerogel. Reproduced with permission.[93] Copyright 2014, Wiley-VCH. b) The adsorption kinetics of hybrid microscopic dimensional melamine-based foams towards water and acetone. Reproduced with permission.[39] Copyright 2016, Royal Society of Chemistry. c,d) The demonstration of high thermal tolerance in air and excellent mechanical flexibility of superhydrophobic and magnetic quartz fibers. Reproduced with permission.[40] Copyright 2016, American Chemical Society.

liquid/liquid interface, hence either hydrophobic/oleophilic, oleophobic/hydrophilic, hydrophilic/underwater-oleophobic or oleophilic/under-oil-hydrophobic materials can be employed. For example, Li et al.[112] demonstrated that the carbon fibers based superhydrophobic aerogels can selectively block the water penetration during separation. Interestingly, after lighting in air after impregnation with hexane, the resultant materials converted to superhydrophilic/underwater-superoleophobic due to the introduction of hydrophilic oxygen-containing groups, enabling the oil/water separation in a contrary direction.

To justify the advantages of magnetic 3D-SPMAs overwhelming other materials in oil/water separation, the exploration of special functions incurred by the magnetic properties is essential. Very recently, Dudchenko et al.[121] demonstrated that magnetic Fe_3O_4 nano-powder based Pickering emulsion could achieve a fouling-free separation process coupling with superhydrophobic membranes, where the magnetic materials were used to convert original oil/water mixture into Pickering emulsion and thus reducing irreversible membrane fouling. Moreover, after use, the nano-magnetite could be simply recycled by magnetic separation. However, although many 3D-SPMAs have been applied in oil/water separation,[34,39,40,104,112] no work has utilize special characters, i.e., magnetic properties of them. Hence, one big challenge lies in how to utilize the magnetism of 3D-SPMAs to modulate or enhance the oil/water separation, thus fully exerting the potential of these magnetic materials.

4.1.3. Removal of Dyes and Heavy-Metal Ions

Different from the oil uptake, the adsorption process of dyes and heavy-metal ions usually take place on the solid/liquid interface, which means only the surface area and the surface chemistry are accounted. Therefore, MPs and 3D-SPMAs share the similar adsorption mechanism. To facilitate efficient contact and adsorption in water environment, the adequate hydrophilicity is often required, which is quite different from the case of oil uptake and oil/water separation. The magnetism and the 3D architecture of 3D-SPMAs can facilitate their easy movement and retrieval by either remotely magnetic control or manual control. Hence, it seems the main advantage of 3D-SPMAs is their monolithic architecture and magnetic responsibility accounting for facile recycling.

Actually, only a few works centered on this topic by using "dry" 3D-SPMAs.[43,93,110] For example, Lei et al.[110] fabricated graphene oxide foam/Fe_3O_4 nanocomposite by microwave-plasma CVD (MPCVD) coupling with post co-precipitation. The resultant materials showed high saturation magnetization M_s = 40.8 emu g^{-1} and a maximum adsorption capacity of 258.6 mg/g towards Cr(IV) at pH 2, which was attributed to electrostatic interactions between 3D-SPMAs and adsorbates. In another work,[43] Fe_3O_4 modified graphene oxide sponge with M_s = 4.4 emu g^{-1} was prepared, showing the equilibrium concentration of methylene blue (MB) as high as 526 mg g^{-1} (**Figure 15**a).

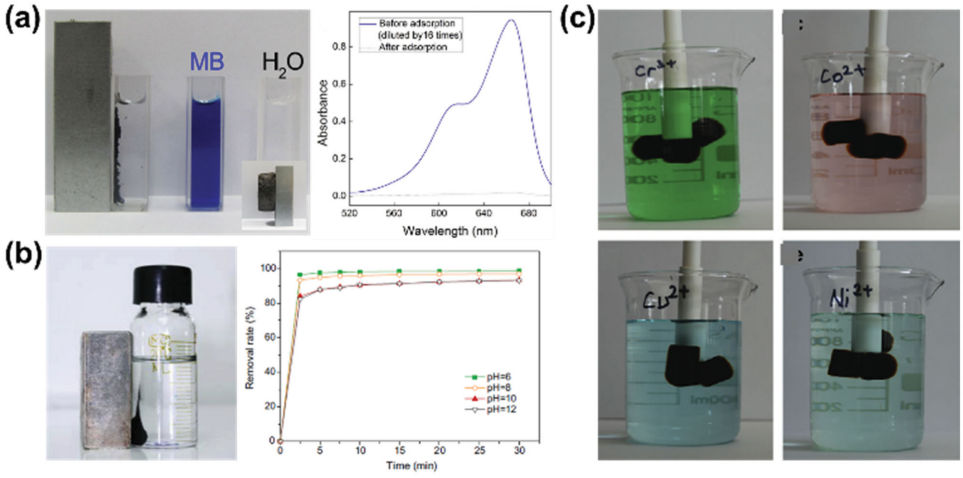

Figure 15. a) The removal of methylene blue by Fe_3O_4/graphene sponge. Reproduced with permission.[43] Copyright 2015, Elsevier. b) Dyes removal by using a magnetic chitosan–Fe(III) hydrogel. Reproduced with permission.[47] Copyright 2011, Elsevier. c) The removal of toxic metal ions by using magnetic p(AMPS) composite hydrogels. Reproduced with permission.[114] Copyright 2009, Elsevier.

4.1.4. Recycling and Regeneration of "Dry" 3D-SPMAs

Considering the cost and environmental sustainability, the recycling ability is another pivotal factor to evaluate the feasibility of materials in practice. In addition, regeneration process may also be accompanied with the extraction of absorbed "pollutants" which might turn into useful stuffs, such as the sources for thermal power generation and fuel cells.

For oil uptake and oil/water separation, four regeneration methods are frequently adopted, i.e., squeezing,[39–41,97,101] distillation/heating,[39,40,112] and combustion,[40,94] and solvent exchange.[4,39,40] Squeezing is adapt to compressible 3D-SPMAs with good mechanical flexibility such as magnetic CNTs sponges and commercial foams derived adsorbents. Extremely simple regeneration procedure as it adopts, the adsorbed solvents, especially the viscous oils are not easy to be removed completely by this process. Besides, large compression strain applied to squeezing often leads to unrecoverable plastic deformation of materials, lowing their cycling performance. Distillation or direct heating is often operated at moderate temperature (typically less than 100 °C), which is capable of removal and collecting adsorbed solvents with relatively low-boiling-point (e.g., chloroform, methanol). For some high-boiling-point and flammable organic solvents and oils (e.g., toluene, crude oil, motor oil), combustion is the best approach if the adsorbents can maintain their structures and properties. However, the extraction of oils is impossible by this approach. Taking advantage of inter-miscibility of most organic solvents and oils, replace the adsorbed organic liquid with another easy-removable one may offer a way to simplify the regeneration procedure or get rid of organic liquids that are difficult to be eliminated. For example,[4] after implementing oil/water separation, the organic solvents in filtering materials could be replaced by low-toxicity and low-boiling-point acetone facilely by acetone flushing. Then the regeneration process is able to be executed by heating with a blower. The whole process is operated in situ, disassembly/reassembly of separation device is not required.

It should be noted that regeneration process may cause the loss of hydrophobicity and magnetic properties of 3D-SPMAs, especially under the extreme conditions such as combustion. On this occasion, a second-round introduction of hydrophobicity and magnetism should be performed. For example, we showed that although magnetic superhydrophobic quartz fibers maintain their 3D networks under extreme high temperature (up to 1150 °C), reloading of magnetic components and/or hydrophobic layer are required to recover their original properties after regeneration by heating/combustion.[40]

For desorption of dyes/metal ions, Yu et al.[43] reported the regeneration of Fe_3O_4 decorated graphene sponge after adsorbing methylene blue by washing with acidic ethanol (pH 2) following with lyophilization. However, a retention capacity of less than 40% was obtained, which might be attributed to the collapse of original porous structures. In addition, the possible leaching of magnetic components, which are usually composed of metals and metal oxides, during acid-involving regeneration processes needs to be taken into account.

4.2. "Dry" 3D-SPMAs for Other Possible Applications

The field of "dry" 3D-SPMAs is a young research area, and therefore many of its potentials have not been fully released. Actually, even in the field of widely studied water remediation, it is still full of challenges and opportunities. In this section, possible and predicted applications of "dry" 3D-SPMAs in water remediation and other fields are discussed.

4.2.1. Water Remediation

The creative and elaborate structural design and chemical composition modulation at both macroscale and microscale offer a huge potential for preparing 3D-SPMAs with distinct advantages in water remediation.

From the view of macroscale structure design, Heiligtag et al.[37] have provided us with quite a few methods to produce materials with diverse structures (Figure 9e). Among those architectures, macroscopic core–shell structures might be very helpful in applications. For instance, a macroscopic magnetic core/nonmagnetic shell architecture is a good choice to protect the magnetic components from falling off or deterioration to some extent. In addition, once the magnetism of materials is too strong, such core/shell architecture can maintain the magnetic-driven properties of materials during use while facilitate separating 3D-SPMAs from magnet after collection. For another consideration, in the field of water remediation by using magnetic powders, one tendency is to devise materials with hydrophilic surface for dispersing in water and hydrophobic core for oil uptake, thus realizing oil spill adsorption submerging water.[77,78,122] 3D-SPMAs faced the same situation. Hydrophobic 3D-SPMAs could adsorb high-density organic solvents underwater by pressing them to the bottom of the water, as demonstrated by many laboratorial works. However, it is impossible to use this in real applications because a huge force is required to overcome the great buoyance of these materials due to their hydrophobicity. Hence, the fabrication of macroscopic hydrophobic core/hydrophilic shell 3D-SPMAs might be useful for treating any kind of oil spills in real condition.

From the standpoint of microscale structure design, it is desirable to fabricate well-defined magnetic structures with tailored magnetic properties. For example, once the magnetic structures possess suitable geometry and sufficient high magnetism, their arrangement might able to be reversibly altered by the applied external magnetic field. Hence, the surface roughness and wettability of 3D-SPMAs could be accordingly manipulated, which is useful for controlled oil/water separation and other separation process.

It is also pivotal to elaborately modulate the chemical composition. For example, in most cases, the adsorption of 3D-SPMAs towards metal ions and dyes showed no obvious selectivity. If the surface chemistry of microstructures is well designed, the 3D-SPMAs will be capable of selective enriching targeted matters.

Apart from the endeavor to promote common performance of water remediation such as adsorption capacity and selectivity, it is equally crucial to investigate other roles of 3D-SPMAs in water remediation. As mentioned in Section 4.1.2., magnetic Fe_3O_4 nanopowder based Pickering emulsion has been produced for fouling-free separation process by coupling with superhydrophobic membranes. Although currently it seems difficult to figure out how to utilize 3D-SPMAs to realize this process, while the work still provide a good hint to inspire us to further investigate possible use of 3D-SPMAs in water remediation. For another example, the property of heat generation from magnetic nanoparticles induced alternative magnetic fields[51] might be used in water remediation. By introducing MNPs with suitable size in 3D networks, the resultant 3D-SPMAs can gain the "remote regeneration" ability in oil uptake. After adsorption of low-melt-point organic solvents, the 3D-SPMAs could be regenerated by subjecting them to the alternative magnetic field, where the adsorbed solvents would be evaporated by AMF-induced heating.

4.2.2. Other Applications

In the first place, certain fundamental studies may expand the applications of 3D-SPMAs. For example, by introducing pores with suitable size in the magnetic shape-memory alloy Ni–Mn–Ga, the resultant foam (**Figure 16**a) showed magnetic-field-induced strain (MFIS) up to 8.7%, which was approaching that of monocrystalline alloy (10%).[35] The large MFIS might be applied in actuators, sensors and energy-harvesting devices. On the other hand, the photocatalysis process might be modulated by magnetic field in 3D-SPMAs.[37] Consequently, The studies of underlying mechanism may promote the understanding of catalysis process and the design of better catalysts.

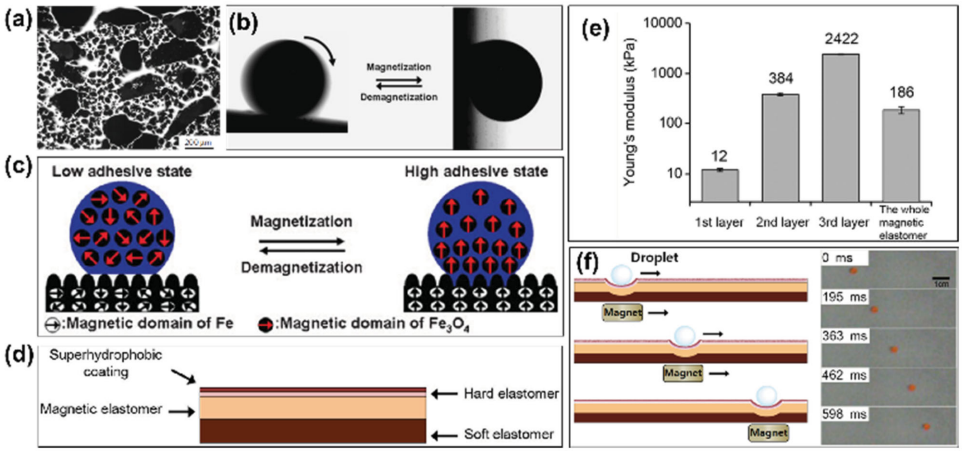

Figure 16. a) The optical micrograph of the polished cross-section of Ni–Mn–Ga foam with a dual pore size. Reproduced with permission.[35] Copyright 2002, Nature Publishing Group. b,c) The magnetic-field-induced reversible adhesion state between superparamagnetic microdroplet and superhydrophobic iron surface, and the corresponding proposed mechanism. Reproduced with permission.[123] Copyright 2008, Wiley-VCH. d–f) The demonstration of configuration, mechanical properties, and practical performance of the superhydrophobic magnetic elastomer actuator. Reproduced with permission.[126] Copyright 2013, Wiley-VCH.

In the second place, the in-field synthesis provided a unique way to modulate structures in 3D-SPMAs, which is feasible to create certain distinctive materials.[36,37] For example, Gish et al. fabricated the silica composite aerogels containing $Nd_2Fe_{14}B$ particles in the presence of magnetic field (Figure 9d). The resultant materials showed pronounced optically anisotropy due to the alignment of magnetic particles in the field during gelation. The resultant materials may found applications in novel optical devices. However, the research on both the preparation and applications exploration of anisotropic 3D-SPMAs is extremely rare.

In the third place, the integration of more properties in 3D-SPMAs could trigger new functions. Cheng et al.[123] showed that the superhydrophobic iron surface can control the wettable state of the superparamagnetic microdroplet with assistance of magnetic field. The magnetized surface can tightly fix the droplet by inducing magnetization of droplet, while release the droplet after demagnetization (Figure 16b,c). This reversible transition enabled a wide range of applications including biochemical separation, no-loss transport of microdroplet, and so on. To extend this switchable process, if the magnetic components are integrated in the thermal-switchable materials (e.g., PNIPAAm films,[124] paraffin/PDMS organogel[125]), then the switching process could be triggered by alternative magnetic field based on AMF-induced thermal effect. Recently, Seo et al.[126] successfully controlled the movement of a normal nonmagnetic water droplet on a specially designed magnetic substrate. As shown in Figure 16d,e, the droplet could be driven by a magnet on the elastomer surface by virtue of local deformation induced by magnetic field. The work demonstrated a novel and interesting actuation style to control the motion of a nonmagnetic droplet in an indirect way. Recently, some electrical conductive 3D-SPMAs have been prepared by either using conductive 3D networks or imparting additional conductive components.[9,127] Once the electrical conductivity is introduced, the magnetic properties could be modulated by applying external voltage, and some interesting properties might appear. The marriage of magnetism with special optical, thermal, and other physicochemical properties might also be beneficial for both fundamental studies and novel applications.

Finally, 3D-SPMAs with strong magnetism may also be used as stirrers or novel bulk catalysts which could be controlled by the magnetic field. It is known that some 3D-SPMAs could be driven to rotate by the common magnetic stirring apparatus.[39] Therefore, they could be directly enrolled into the reaction mixture (gases, solutions, etc.) and serve as stirrers, enhancing the mass transfer of reaction upon the using of magnetic stirring apparatus. If these 3D-SPMAs are anchored with specific catalysts, then they could be visualized as the reaction containers where the reaction takes place. In this way, when placed into the reaction mixture upon using the magnetic stirring apparatus, they would function as both reaction factories and mass transfer enhancer to trigger and accelerate specific chemical process. After reaction, they could be facilely removed by a magnet.

4.3. Hydrogel-Based 3D-SPMAs for Water Remediation

In contrast with "dry" 3D-SPMAs such as sponges and aerogels, the hydrogel-based 3D-SPMAs are often used for remote-control removal of dyes/heavy metal ions, which can be attributed to their innate hydrophilicity and magnetism. However, because the internal cavities of hydrogels are crammed with water, they cannot be applied in oil uptake.

Regarding the water remediation, hydrogel-based 3D-SPMAs are often used to clean dyes and heavy-metal ions by utilizing the versatile interactions between 3D networks of magnetic hydrogels and adsorbates.[47,114,115,128–135] It should be noted since the active sites of 3D networks are surrounded by the water in the initial magnetic hydrogels, hence the remediation process often involve the competitive adsorption between water and pollutants. For instance, magnetic chitosan–Fe(III) hydrogels (Figure 15b) were employed to adsorb a wide range of dyes under alkaline environment (pH 12) with a high maximum adsorption capacity of 294.5 mg g^{-1} (referred to the dry gels).[47] The adsorption mechanism was explained by the complexation of dyes with Fe(III) center by a dye-water exchange process. Ozay et al.[114,115] reported the magnetic hydrogels based on 2-acrylamido-2-methyl-1-propansulfonic acid (AMPS) or poly(2-acrylamido-2-methyl-1-propansulfonic acid-co-vinylimidazole) by photopolymerization. The resultant hydrogels can adsorb a wide range of metal ions including Cu(II), Cd(II), Fe(II), Pb(II), Ni(II), Cu(II) and Cr(III) from aqueous environment (Figure 15c). After use, they can be regenerated by desorbing in weakly acid media. More importantly, all of them merited the facile separation process by a magnet.

From the aspect of desorption and regeneration, solution of alkali, acid, and neutral salts are often used to break the interactions of adsorbates and adsorbents, and replace adsorption sites.[47,114,115,128,129] Followed rinsing with water or other solution enables the recovery of adsorbents readily for next-round adsorption. For example, NaOH aqueous solution (approximately 0.05 to 1 mol L^{-1}) was used to desorb diverse adsorbed dyes from chitosan-Fe(III) hydrogel with a efficiency over 90%.[47] After desorption, adsorbents were rinsed with 0.1 mol L^{-1} HCl to accomplish regeneration process. In another work, Ozay et al.[115] demonstrated the elution of adsorbed toxic metal ions on p(AMPS) hydrogels by soaking in diverse acids. They found H_2SO_4 (0.1 mol L^{-1}) is the best choice to regenerate hydrogels, because of combined high desorption efficiency (up to five cycles over 75% desorption ratio) and minimal effect on magnetic properties of materials. In contrast, HNO_3 and HCl eliminated magnetic response of hydrogels after three or four adsorption–desorption cycles. This result points the importance of careful selection of eluents so as to maintain the properties of adsorbents.

4.4. Hydrogel-Based 3D-SPMAs for Other Applications

Hydrogel-based 3D-SPMAs have also found many other useful applications apart from water remediation, such as controlled drug release, magnetic-field-controlled thermal therapy, and so on. Several typical applications of hydrogel-based 3D-SPMAs are reviewed in this section. Readers who are interested in more details about biomedical applications of magnetic hydrogels could refer to another excellent review.[54]

The excellent biocompatibility of hydrogels allowed their diverse applications in biological areas. The magnetism

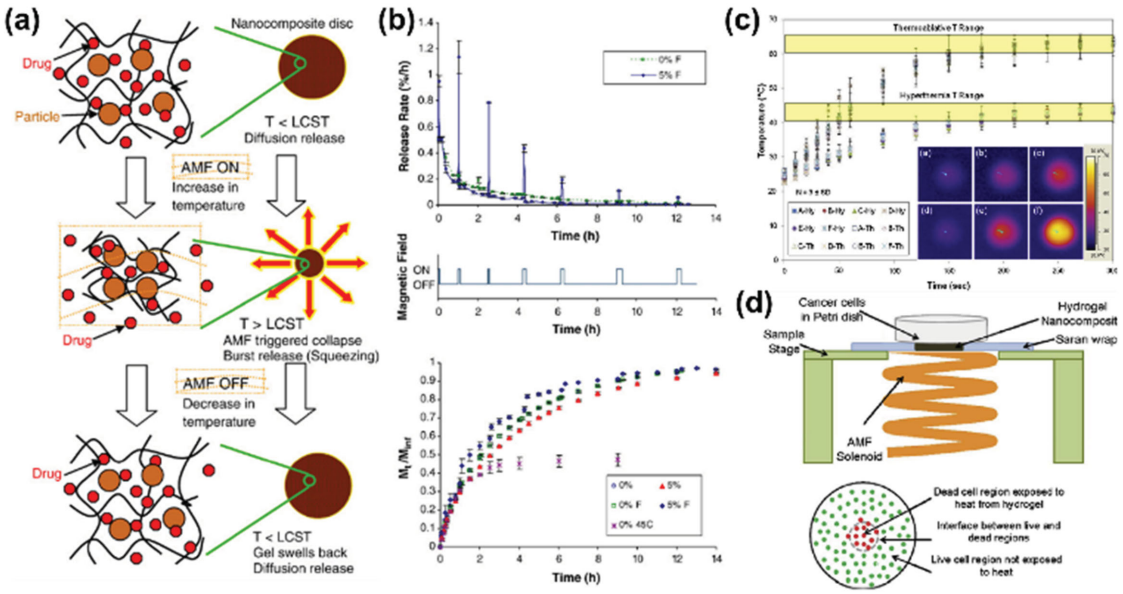

Figure 17. a,b) Schematic illustration of the effect of ON–OFF cycles of alternating magnetic field (AMF) to the magnetic nanocomposites of NIPAAm, and the use of them for controlled release of Vitamin B12. Reproduced with permission.[49] Copyright 2008, Elsevier. c,d) Thermal analysis of poly(ethylene glycol)-based magnetic hydrogel nanocomposites exposed to varied AMF strengths to control gel temperatures in the hyperthermia or thermoablative temperature ranges, and the configuration of the apparatus for conducting in vitro cancer therapy. Reproduced with permission.[116] Copyright 2009, Elsevier.

integration further expands their functions. For example, hydrogel-based 3D-SPMAs have been widely applied into tissue engineering, drug delivery, enzyme immobilization, and cancer therapy.[49,54,116,117,136–139] In this field, the remotely heatable property of magnetic nanoparticles (MNPs) is frequently used. In detail, the MNPs can generate heat locally under the external AMF due to the hysteretic losses as characterized by M-H diagrams,[51] which was just like the energy dissipation behavior in sponges under compression cycles. In this way, one can remotely and locally heat the 3D-SPMAs and thus realizing specific applications.

It is important to feed drugs at specific position in a controllable manner, so as to maximize the efficiency of drugs and avoid unfavorable effects. Encapsulation of drugs in a stimuli-responsive frameworks can serve as a good way to control the release by applying appropriate stimuli. Combining the biocompatibility of hydrogels and AMF-induced heat generation property of MNPs, the hydrogel-based 3D-SPMAs can provide remote controllability in drug release. For example, Satarkar et al.[49] incorporated superparamagnetic Fe_3O_4 particles in poly(*N*-isopropylacrylamide) (PNiPAAm) hydrogels. Thanks to the negative temperature sensitiveness of PNiPAAm, the 3D frameworks shrank with increasing temperature induced by AMF and thus squeezing drugs out of gels. When AMF was removed, hydrogels swelled back and the drug release was suppressed (**Figure 17**a,b). In this way, the magnetic hydrogels enabled an interesting pulsatile drug release behaviour, which is important for applications in externally actuated drug delivery systems. For another example, magnetic hydrogels was employed for cancer therapy by hyperthermia. Meenach and co-workers presented a poly(ethylene glycol)-based magnetic hydrogel nanocomposites via free radical polymerization in the presence of iron oxide nanoparticles.[116] The hydrogel can reach either hyperthermic temperatures (approximately 41 to 45 °C) or thermoablative temperatures (>50 °C) upon exposure to AMF with appropriate parameters (Figure 17c,d), and their abilities of in vitro killing M059K glioblastoma cells has been demonstrated.

In addition to biomedical applications, the hydrogel-based 3D-SPMAs can also be applied in other fields (**Figure 18**).[46,48,50,119,140] For example, the PNiPAAm/Fe_3O_4 hydrogel was applied in microfluidic devices,[48] which served as an AMF-controlled valve that utilizes the reversible swell/collapse behavior of hydrogels responding to low/high temperatures. In another work, Ramanujan et al.[50] prepared macroscopic polyvinyl alcohol/Fe_3O_4 ferrogel that can simulate the artificial finger by applying appropriate magnetic field. In another work, combining the self-healing behavior of Schiff-base linkage in chitosan-based hydrogels and magnetism endowed by Fe_3O_4 nanoparticles, Zhang et al.[46] reported an interesting magnetic self-healing hydrogel which could be easily gathered and passed through narrow channels directed by a magnet. The presented self-healing behaviour is useful to repair the fragmented macroscopic 3D architecture of hydrogels, which is important for facile collection and regeneration of materials.

4.5. Pros and Cons of 3D-SPMAs in Water Remediation

Until now, water remediation is one of the most promising and widely studied applications of 3D-SPMAs, especially the "dry" 3D-SPMAs. Compared with nonmagnetic 3D-SPAs, their magnetic properties endow them with excellent controllability in oil uptake and dye/metal ions adsorption, leading to much simplified process in orientated adsorption and retrieval. In

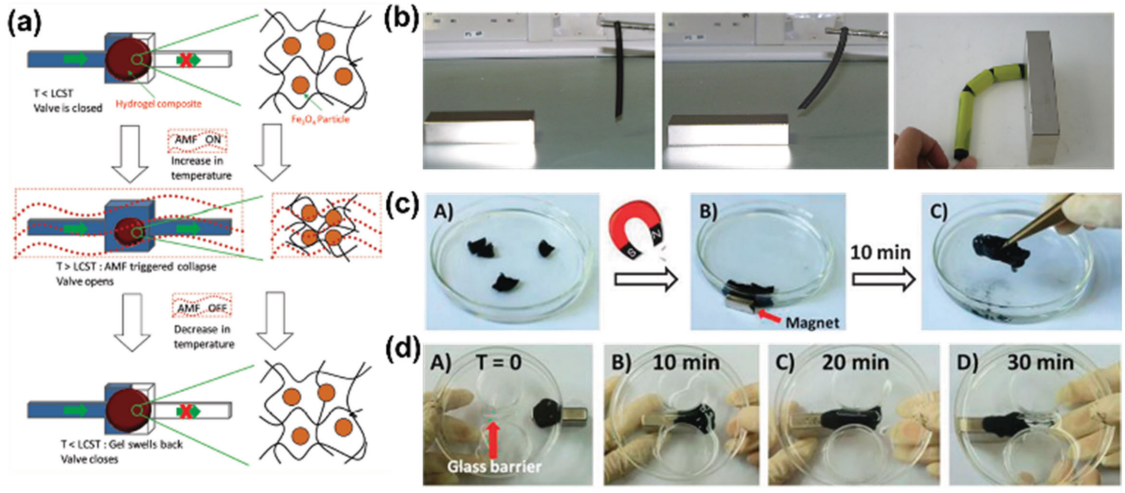

Figure 18. a) Schematic illustration of the operation mechanism of remote controlled PNIPAAm/Fe_3O_4 hydrogel nanocomposite valves by an alternating magnetic field. Reproduced with permission.[48] Copyright 2009, Royal Society of Chemistry. b) The demonstration of magnetic field triggered actuation of polyvinyl alcohol/Fe_3O_4 ferrogel. Reproduced with permission.[50] Copyright 2006, Institute of Physics (IOP) publishing. c–d) The demonstration of the magnetic-field-induced recombination process and barrier crossing process of a magnetic self-healing hydrogel. Reproduced with permission.[46] Copyright 2012, Royal Society of Chemistry.

comparison with fragmented MPs, 3D-SPMAs' eminent porosities and self-supporting structures ensure their large adsorption capacity, and enable their practical use in large-scale without need to consider the difficulty in complete retrieval.

However, it seems that magnetic controllability serves the only merit of 3D-SPMAs in water remediation, at least the exclusively studied one currently. In this regard, the advantage of 3D-SPMAs may not be sufficient enough to validate their overwhelming superiority in this realm. Especially, the uniqueness of magnetic properties in oil/water separation is seldom explored. In the second place, the integration of magnetism is often at the cost of performance wane, such as decreased mass-normalized adsorption capacity in oil uptake. This is attributed to that magnetic components are always "heavy" substances, and they often have nothing to do with adsorption/separation process. Thirdly, the stability of magnetism under certain environmental parameters (e.g., temperature, pH) remains to be addressed.

Therefore, the pros and cons of 3D-SPMAs in water remediation point the efforts needed to be put in this realm, i.e., to overcome the intrinsic issues of integrated magnetic components (e.g., sacrificed performance, instability), and to explore other unique functions in applications.

5. Conclusion and Perspective

In past few years, 3D self-supporting porous magnetic assemblies have appeared as rising stars in a wide range of applications. The free-standing architectures, 3D cellular networks, high surface areas, and magnetic responsiveness endow them with unique advantages in water remediation and beyond, such as remotely controlled oil uptake, magnetic retrieval or separation after use, no-loss transport of microdroplet, magnetism-triggered sensors, remotely controlled drug release, the preparation of optically anisotropic bulk materials, and so on. These encouraging results have stimulated the vast passion for investigating 3D-SPMAs from the aspect of both syntheses and applications.

In this article, the field of 3D-SPMAs, including synthetic strategies and applications (especially in water remediation) has been comprehensively reviewed. The fundamental knowledge of magnetic materials, magnetic powders, 3D self-supporting porous magnetic assemblies, and wettability have been introduced at first. Then the synthetic strategies of 3D-SPMAs were concluded based on "dry" 3D-SPMAs and "wet" 3D-SPMAs. The pros and cons of the corresponding methods have also been discussed in depth. Finally, the applications of 3D-SPMAs, especially in water remediation have been reviewed, where the working mechanism and design principles have been analyzed. Additional possible applications, and predicted potential applications of 3D-SPMAs have also been discussed.

Until now, the field of 3D-SPMAs is still a young and energetic research area full of opportunities and challenges. Although a number of scientists have devoted themselves to this field and 3D-SPMAs have been widely employed in water remediation and other fields, more efforts are required to develop efficient and cost-effective synthetic strategies for 3D-SPMAs, as well as to fully utilize their unique properties and release their potential to fulfil the requirements of practical applications. Herein, some key challenges in this field are proposed as follows:

1) Maximization and release of the potential of magnetic components in 3D-SPMAs. In certain cases, e.g., the oil uptake, the integration of magnetic components without elaborate design can cause the performance deterioration of materials. Hence, the subtly control the magnetic components by chemical modification, morphology engineering and others means can enhance the performance or impart new functions in materials, such as improved water/oil selectivity, adsorption speed, and specific enrichment of target matters. On

the other hand, in many applications, the unique magnetic features of 3D-SPMAs should be considered to enhance the performance or modulate properties of materials. For example, the separation process might be modulated or even reversed by using 3D-SPMAs under specific magnetic fields.

2) The structure control of 3D-SPMAs at both macroscale and microscale. Many physical properties and application performance of materials are highly dependent on their structures. By macroscale structure control, one can devise macroscopic core/shell structure, such as magnetic core/nonmagnetic shell and hydrophobic core/hydrophilic shell, for protecting the magnetic components and treating the submerged oil. By microscale structure engineering of magnetic components, it might be possible to remotely modulate the wettability of 3D-SPMAs for water remediation and other novel applications.
3) The introduction of additional functions in 3D-SPMAs. The marriage of magnetism with other properties such as electrical conductivity, self-healing properties, and high thermostability in 3D-SPMAs can be achieved by either integrating functional components or selecting appropriate 3D networks. To this end, the resultant materials can display diverse functions and enhanced performance in water remediation and beyond, such as electrical-modulated wettability, facile retrieval process, and extraordinary temperature tolerance.
4) The development of facile and creative methods for materials preparation. The realization of specific functions depends on the development of effective fabrication strategies. Certain inspiring methods, such as anisotropic macroscopic structures design, microscopic structures engineering, in-field preparation, adsorption/combustion preparation process, etc., are of great importance to develop 3D-SPMAs with unique properties and high performance-to-cost ratio.

To sum up, currently, the field of 3D-SPMAs is far from maturation, coexisting huge challenges and opportunities. We believe that in light of the joint efforts from researchers of different backgrounds including materials science, chemistry, physics, biology, etc., diverse 3D-SPMAs with enhanced performance and expanded application territory will be rapidly developed. In this way, 3D-SPMAs will undoubtedly make a big difference in materials science in the near future.

Acknowledgements

This work was supported by NSFC (21233001, 21129001, 51272006, 51121091 and 51432002) and MOST (2011CB932601).

Received: March 1, 2016
Revised: March 11, 2016
Published online: April 28, 2016

[1] Y. Gao, Y. S. Zhou, W. Xiong, M. Wang, L. Fan, H. Rabiee-Golgir, L. Jiang, W. Hou, X. Huang, L. Jiang, *ACS Appl. Mater. Interfaces* **2014**, *6*, 5924.
[2] C. Ruan, K. Ai, X. Li, L. Lu, *Angew. Chem. Int. Ed.* **2014**, *53*, 5556.
[3] Y. Wang, Y. Shi, L. Pan, M. Yang, L. Peng, S. Zong, Y. Shi, G. Yu, *Nano Lett.* **2014**, *14*, 4803.
[4] R. Du, X. Gao, Q. Feng, Q. Zhao, P. Li, S. Deng, L. Shi, J. Zhang, *Adv. Mater.* **2016**, *28*, 936.
[5] X. Gao, J. Zhou, R. Du, Z. Xie, S. Deng, R. Liu, Z. Liu, J. Zhang, *Adv. Mater.* **2016**, *28*, 168.
[6] S. Chen, G. He, H. Hu, S. Jin, Y. Zhou, Y. He, S. He, F. Zhao, H. Hou, *Energy Environ. Sci.* **2013**, *6*, 2435.
[7] C. Wu, X. Huang, X. Wu, R. Qian, P. Jiang, *Adv. Mater.* **2013**, *25*, 5658.
[8] H. Bi, Z. Yin, X. Cao, X. Xie, C. Tan, X. Huang, B. Chen, F. Chen, Q. Yang, X. Bu, X. Lu, L. Sun, H. Zhang, *Adv. Mater.* **2013**, *25*, 5916.
[9] X. Zhou, Z. Zhang, X. Xu, X. Men, X. Zhu, *Ind. Eng. Chem. Res.* **2013**, *52*, 9411.
[10] X. Gui, J. Wei, K. Wang, A. Cao, H. Zhu, Y. Jia, Q. Shu, D. Wu, *Adv. Mater.* **2010**, *22*, 617.
[11] Y. Zhao, C. Hu, Y. Hu, H. Cheng, G. Shi, L. Qu, *Angew. Chem.* **2012**, *124*, 11533.
[12] R. Du, N. Zhang, J. H. Zhu, Y. Wang, C. Y. Xu, Y. Hu, N. N. Mao, H. Xu, W. J. Duan, L. Zhuang, L. T. Qu, Y. L. Hou, J. Zhang, *Small* **2015**, *11*, 3903.
[13] R. Du, Q. Zhao, N. Zhang, J. Zhang, *Small* **2015**, *11*, 3263.
[14] Y. Wu, N. Yi, L. Huang, T. Zhang, S. Fang, H. Chang, N. Li, J. Oh, J. A. Lee, M. Kozlov, A. C. Chipara, H. Terrones, P. Xiao, G. Long, Y. Huang, F. Zhang, L. Zhang, X. Lepró, C. Haines, M. D. Lima, N. P. Lopez, L. P. Rajukumar, A. L. Elias, S. Feng, S. J. Kim, N. T. Narayanan, P. M. Ajayan, M. Terrones, A. Aliev, P. Chu, Z. Zhang, R. H. Baughman, Y. Chen, *Nat. Commun.* **2015**, *6*, 6141.
[15] L. Chen, R. Du, J. Zhang, T. Yi, *J. Mater. Chem. A* **2015**, *3*, 20547.
[16] R. Du, N. Zhang, H. Xu, N. Mao, W. Duan, J. Wang, Q. Zhao, Z. Liu, J. Zhang, *Adv. Mater.* **2014**, *26*, 8053.
[17] R. Du, Z. Zheng, N. Mao, N. Zhang, W. Hu, J. Zhang, *Adv. Sci.* **2015**, *2*, 1400006.
[18] D. Zang, C. Wu, R. Zhu, W. Zhang, X. Yu, Y. Zhang, *Chem. Commun.* **2013**, *49*, 8410.
[19] S.-J. Choi, T.-H. Kwon, H. Im, D.-I. Moon, D. J. Baek, M.-L. Seol, J. P. Duarte, Y.-K. Choi, *ACS Appl. Mater. Interfaces* **2011**, *3*, 4552.
[20] R. Du, Y. Xu, Y. Luo, X. Zhang, J. Zhang, *Chem. Commun.* **2011**, *47*, 6287.
[21] R. Du, X.-t. Zhang, *Acta Phys. Chim. Sin.* **2012**, *28*, 2305.
[22] Q. Jiuhui, *J. Environ. Sci.* **2008**, *20*, 1.
[23] Y. Sharma, V. Srivastava, V. Singh, S. Kaul, C. Weng, *Environ. Technol.* **2009**, *30*, 583.
[24] M. M. Khin, A. S. Nair, V. J. Babu, R. Murugan, S. Ramakrishna, *Energy Environ. Sci.* **2012**, *5*, 8075.
[25] O. V. Kharissova, H. R. Dias, B. I. Kharisov, *RSC Adv.* **2015**, *5*, 6695.
[26] S. Nagappan, C.-S. Ha, *J. Mater. Chem. A* **2015**, *3*, 3224.
[27] G. Giakisikli, A. N. Anthemidis, *Anal. Chim. Acta* **2013**, *789*, 1.
[28] C. Herrero-Latorre, J. Barciela-García, S. García-Martín, R. Peña-Crecente, J. Otárola-Jiménez, *Anal. Chim. Acta* **2015**, *892*, 10.
[29] A.-F. Ngomsik, A. Bee, M. Draye, G. Cote, V. Cabuil, *C. R. Chim.* **2005**, *8*, 963.
[30] C. T. Yavuz, A. Prakash, J. Mayo, V. L. Colvin, *Chem. Eng. Sci.* **2009**, *64*, 2510.
[31] R. D. Ambashta, M. Sillanpää, *J. Hazard. Mater.* **2010**, *180*, 38.
[32] S. C. Tang, I. M. Lo, *Water Res.* **2013**, *47*, 2613.
[33] P. Calcagnile, D. Fragouli, I. S. Bayer, G. C. Anyfantis, L. Martiradonna, P. D. Cozzoli, R. Cingolani, A. Athanassiou, *ACS Nano* **2012**, *6*, 5413.
[34] L. Wu, L. Li, B. Li, J. Zhang, A. Wang, *ACS Appl. Mater. Interfaces* **2015**, *7*, 4936.
[35] M. Chmielus, X. Zhang, C. Witherspoon, D. Dunand, P. Müllner, *Nat. Mater.* **2009**, *8*, 863.
[36] M. Gich, L. Casas, A. Roig, E. Molins, J. Sort, S. Surinach, M. Baró, J. Munoz, L. Morellon, M. Ibarra, *Appl. Phys. Lett.* **2003**, *82*, 4307.

[37] F. J. Heiligtag, M. J. A. Leccardi, D. Erdem, M. J. Süess, M. Niederberger, *Nanoscale* **2014**, *6*, 13213.
[38] N. Chen, Q. Pan, *ACS Nano* **2013**, *7*, 6875.
[39] R. Du, Q. Feng, H. Ren, Q. Zhao, X. Gao, J. Zhang, *J. Mater. Chem. A* **2016**, *4*, 938.
[40] R. Du, Q. Zhao, P. Li, H. Ren, X. Gao, J. Zhang, *ACS Appl. Mater. Interfaces* **2016**, *8*, 1025.
[41] X. Gui, Z. Zeng, Z. Lin, Q. Gan, R. Xiang, Y. Zhu, A. Cao, Z. Tang, *ACS Appl. Mater. Interfaces* **2013**, *5*, 5845.
[42] S. Zhou, W. Jiang, T. Wang, Y. Lu, *Ind. Eng. Chem. Res.* **2015**, *54*, 5460.
[43] B. Yu, X. Zhang, J. Xie, R. Wu, X. Liu, H. Li, F. Chen, H. Yang, Z. Ming, S.-T. Yang, *Appl. Surf. Sci.* **2015**, *351*, 765.
[44] L. Wu, J. Zhang, B. Li, A. Wang, *Polym. Chem.* **2014**, *5*, 2382.
[45] T. Li, H. Liu, L. Zeng, S. Yang, Z. Li, J. Zhang, X. Zhou, *J. Mater. Chem.* **2011**, *21*, 12865.
[46] Y. Zhang, B. Yang, X. Zhang, L. Xu, L. Tao, S. Li, Y. Wei, *Chem. Commun.* **2012**, *48*, 9305.
[47] C. Shen, Y. Shen, Y. Wen, H. Wang, W. Liu, *Water Res.* **2011**, *45*, 5200.
[48] N. S. Satarkar, W. Zhang, R. E. Eitel, J. Z. Hilt, *Lab Chip* **2009**, *9*, 1773.
[49] N. S. Satarkar, J. Z. Hilt, *J. Controlled Release* **2008**, *130*, 246.
[50] R. Ramanujan, L. Lao, *Smart Mater. Struct.* **2006**, *15*, 952.
[51] G. Glöckl, R. Hergt, M. Zeisberger, S. Dutz, S. Nagel, W. Weitschies, *J. Phys.: Condens. Matter* **2006**, *18*, S2935.
[52] R. K. Upadhyay, N. Soin, S. S. Roy, *RSC Adv.* **2014**, *4*, 3823.
[53] Z. Xue, Y. Cao, N. Liu, L. Feng, L. Jiang, *J. Mater. Chem. A* **2014**, *2*, 2445.
[54] Y. Li, G. Huang, X. Zhang, B. Li, Y. Chen, T. Lu, T. J. Lu, F. Xu, *Adv. Funct. Mater.* **2013**, *23*, 660.
[55] O. Knop, K. Reid, Sutarno, Y. Nakagawa, *Can. J. Chem.* **1968**, *46*, 3463.
[56] J. Chen, C. Sorensen, K. Klabunde, G. Hadjipanayis, E. Devlin, A. Kostikas, *Phys. Rev.B* **1996**, *54*, 9288.
[57] W. Miao, J. Ding, P. McCormick, R. Street, *J. Alloys Compd.* **1996**, *240*, 200.
[58] P. Brown, L. J. Hope-Weeks, *J. Sol–Gel Sci. Technol.* **2009**, *51*, 238.
[59] U. Topal, H. I. Bakan, *Mater. Chem. Phys.* **2010**, *123*, 121.
[60] H. Danan, A. Herr, A. Meyer, *J. Appl. Phys.* **1968**, *39*, 669.
[61] J. Ding, T. Reynolds, W. Miao, P. McCormick, R. Street, *Appl. Phys. Lett.* **1994**, *65*, 3135.
[62] H.-P. Cong, X.-C. Ren, P. Wang, S.-H. Yu, *ACS Nano* **2012**, *6*, 2693.
[63] L. Wu, Q. Li, C. H. Wu, H. Zhu, A. Mendoza-Garcia, B. Shen, J. Guo, S. Sun, *J. Am. Chem. Soc.* **2015**, *137*, 7071.
[64] G. Herzer, *IEEE Trans. Magn.* **1990**, *26*, 1397.
[65] Y.-w. Jun, Y.-M. Huh, J.-s. Choi, J.-H. Lee, H.-T. Song, S. Kim, S. Yoon, K.-S. Kim, J.-S. Shin, *J. Am. Chem. Soc.* **2005**, *127*, 5732.
[66] X. Gui, Z. Zeng, Y. Zhu, H. Li, Z. Lin, Q. Gan, R. Xiang, A. Cao, Z. Tang, *Adv. Mater.* **2014**, *26*, 1248.
[67] A. Marmur, *Langmuir* **2003**, *19*, 8343.
[68] Y. Tian, B. Su, L. Jiang, *Adv. Mater.* **2014**, *26*, 6872.
[69] K.-Y. Law, *J. Phys. Chem. Lett.* **2014**, *5*, 686.
[70] R. Blossey, *Nat. Mater.* **2003**, *2*, 301.
[71] A. Lafuma, D. Quéré, *Nat. Mater.* **2003**, *2*, 457.
[72] R. N. Wenzel, *Ind. Eng. Chem.* **1936**, *28*, 988.
[73] A. Cassie, S. Baxter, *Trans. Faraday Soc.* **1944**, *40*, 546.
[74] R. Kaur, A. Hasan, N. Iqbal, S. Alam, M. K. Saini, S. K. Raza, *J. Sep. Sci.* **2014**, *37*, 1805.
[75] Z. Sun, L. Wang, P. Liu, S. Wang, B. Sun, D. Jiang, F. S. Xiao, *Adv. Mater.* **2006**, *18*, 1968.
[76] Q. Zhu, F. Tao, Q. Pan, *ACS Appl. Mater. Interfaces* **2010**, *2*, 3141.
[77] A. Abbaspourrad, N. J. Carroll, S. H. Kim, D. A. Weitz, *Adv. Mater.* **2013**, *25*, 3215.
[78] A. Pavía-Sanders, S. Zhang, J. A. Flores, J. E. Sanders, J. E. Raymond, K. L. Wooley, *ACS Nano* **2013**, *7*, 7552.
[79] R. T. Olsson, M. A. Samir, G. Salazar-Alvarez, L. Belova, V. Ström, L. A. Berglund, O. Ikkala, J. Nogues, U. W. Gedde, *Nat. Nanotechnol.* **2010**, *5*, 584.
[80] G. Davies, S. Zhen, *J. Mater. Sci* **1983**, *18*, 1899.
[81] J. Banhart, *Prog. Mater. Sci.* **2001**, *46*, 559.
[82] D. Gao, G. Yang, Z. Zhu, J. Zhang, Z. Yang, Z. Zhang, D. Xue, *J. Mater. Chem.* **2012**, *22*, 9462.
[83] B. C. Tappan, S. A. Steiner, E. P. Luther, *Angew. Chem. Int. Ed.* **2010**, *49*, 4544.
[84] P. Jiang, J. Cizeron, J. F. Bertone, V. L. Colvin, *J. Am. Chem. Soc.* **1999**, *121*, 7957.
[85] B. Tappan, M. Huynh, M. Hiskey, D. Chavez, E. Luther, J. Mang, S. Son, *J. Am. Chem. Soc.* **2006**, *128*, 6589.
[86] N. C. Bigall, A. K. Herrmann, M. Vogel, M. Rose, P. Simon, W. Carrillo-Cabrera, D. Dorfs, S. Kaskel, N. Gaponik, A. Eychmüller, *Angew. Chem. Int. Ed.* **2009**, *48*, 9731.
[87] I. Vukovic, S. Punzhin, Z. Vukovic, P. Onck, J. T. M. De Hosson, G. ten Brinke, K. Loos, *ACS Nano* **2011**, *5*, 6339.
[88] W. Liu, P. Rodriguez, L. Borchardt, A. Foelske, J. Yuan, A. K. Herrmann, D. Geiger, Z. Zheng, S. Kaskel, N. Gaponik, *Angew. Chem. Int. Ed.* **2013**, *52*, 9849.
[89] D. Wen, A.-K. Herrmann, L. Borchardt, F. Simon, W. Liu, S. Kaskel, A. Eychmüller, *J. Am. Chem. Soc.* **2014**, *136*, 2727.
[90] N. Leventis, N. Chandrasekaran, A. G. Sadekar, C. Sotiriou-Leventis, H. Lu, *J. Am. Chem. Soc.* **2009**, *131*, 4576.
[91] U. Topal, H. I. Bakan, *J. Eur. Ceram. Soc.* **2010**, *30*, 3167.
[92] Y. Chu, Q. Pan, *ACS Appl. Mater. Interfaces* **2012**, *4*, 2420.
[93] B. Kong, J. Tang, Z. Wu, J. Wei, H. Wu, Y. Wang, G. Zheng, D. Zhao, *Angew. Chem. Int. Ed.* **2014**, *53*, 2888.
[94] B. Ge, Z. Zhang, X. Zhu, G. Ren, X. Men, X. Zhou, *Colloids Surf., A* **2013**, *429*, 129.
[95] S. F. Chin, A. N. B. Romainor, S. C. Pang, *Mater. Lett.* **2014**, *115*, 241.
[96] W. Chen, S. Li, C. Chen, L. Yan, *Adv. Mater.* **2011**, *23*, 5679.
[97] A. Turco, C. Malitesta, G. Barillaro, A. Greco, A. Maffezzoli, E. Mazzotta, *J. Mater. Chem. A* **2015**, *3*, 17685.
[98] Z. Jiang, L. D. Tijing, A. Amarjargal, C. H. Park, K.-J. An, H. K. Shon, C. S. Kim, *Composites, Part B: Engineering* **2015**, *77*, 311.
[99] C. Cannas, M. F. Casula, G. Concas, A. Corrias, D. Gatteschi, A. Falqui, A. Musinu, C. Sangregorio, G. Spano, *J. Mater. Chem.* **2001**, *11*, 3180.
[100] D. Carta, M. F. Casula, A. Corrias, A. Falqui, D. Loche, G. Mountjoy, P. Wang, *Chem. Mater.* **2009**, *21*, 945.
[101] L. Li, B. Li, L. Wu, X. Zhao, J. Zhang, *Chem. Commun.* **2014**, *50*, 7831.
[102] P. Thanikaivelan, N. T. Narayanan, B. K. Pradhan, P. M. Ajayan, *Sci. Rep.* **2012**, *2*.
[103] L. Chen, B. Wei, X. Zhang, C. Li, *Small* **2013**, *9*, 2331.
[104] J. Li, L. Shi, Y. Chen, Y. Zhang, Z. Guo, B.-l. Su, W. Liu, *J. Mater. Chem.* **2012**, *22*, 9774.
[105] B. Ge, X. Zhu, Y. Li, X. Men, P. Li, Z. Zhang, *Colloids Surf. A* **2015**, *482*, 687.
[106] S. Liu, Q. Xu, S. S. Latthe, A. B. Gurav, R. Xing, *RSC Adv.* **2015**, *5*, 68293.
[107] Y. Yang, Z. Liu, J. Huang, C. Wang, *J. Mater. Chem. A* **2015**, *3*, 5875.
[108] Q. Zhu, Q. Pan, F. Liu, *J. Phys. Chem. C* **2011**, *115*, 17464.
[109] S. Liu, Q. Yan, D. Tao, T. Yu, X. Liu, *Carbohydr. Polym.* **2012**, *89*, 551.
[110] Y. Lei, F. Chen, Y. Luo, L. Zhang, *J. Mater. Sci.* **2014**, *49*, 4236.
[111] S. Yang, L. Chen, L. Mu, P.-C. Ma, *J. Colloid Interface Sci.* **2014**, *430*, 337.

[112] Y. Li, X. Zhu, B. Ge, X. Men, P. Li, Z. Zhang, *Appl. Phys. A* **2015**, *120*, 949.
[113] C. Liu, J. Yang, Y. Tang, L. Yin, H. Tang, C. Li, *Colloids Surf., A* **2015**, *468*, 10.
[114] O. Ozay, S. Ekici, Y. Baran, N. Aktas, N. Sahiner, *Water Res.* **2009**, *43*, 4403.
[115] O. Ozay, S. Ekici, Y. Baran, S. Kubilay, N. Aktas, N. Sahiner, *Desalination* **2010**, *260*, 57.
[116] S. A. Meenach, J. Z. Hilt, K. W. Anderson, *Acta Biomater.* **2010**, *6*, 1039.
[117] G. Giani, S. Fedi, R. Barbucci, *Polymers* **2012**, *4*, 1157.
[118] R. Messing, N. Frickel, L. Belkoura, R. Strey, H. Rahn, S. Odenbach, A. M. Schmidt, *Macromolecules* **2011**, *44*, 2990.
[119] P. Ilg, *Soft Matter* **2013**, *9*, 3465.
[120] Y. Yang, Z. Liu, J. Huang, C. Wang, *J. Mater. Chem. A* **2015**, *3*, 5875.
[121] A. V. Dudchenko, J. Rolf, L. Shi, L. Olivas, W. Duan, D. Jassby, *ACS Nano* **2015**, *9*, 9930.
[122] J. A. Flores, A. Pavía-Sanders, Y. Chen, D. J. Pochan, K. L. Wooley, *Chem. Mater.* **2015**, *27*, 3775.
[123] Z. Cheng, L. Feng, L. Jiang, *Adv. Funct. Mater.* **2008**, *18*, 3219.
[124] T. Sun, G. Wang, L. Feng, B. Liu, Y. Ma, L. Jiang, D. Zhu, *Angew. Chem. Int. Ed.* **2004**, *43*, 357.
[125] X. Yao, J. Ju, S. Yang, J. Wang, L. Jiang, *Adv. Mater.* **2014**, *26*, 1895.
[126] K. Seo, R. Wi, S. Im, D. Kim, *Polym. Adv. Technol.* **2013**, *24*, 1075.
[127] Y. Xue, Y. Yang, H. Sun, X. Li, S. Wu, A. Cao, H. Duan, *Adv. Mater.* **2015**, *27*, 7241.
[128] S. C. Tang, P. Wang, K. Yin, I. M. Lo, *Environ. Eng. Sci.* **2010**, *27*, 947.
[129] P. Rao, I. M. Lo, K. Yin, S. C. Tang, *J. Environ. Manage.* **2011**, *92*, 1690.
[130] Z. Liu, H. Wang, C. Liu, Y. Jiang, G. Yu, X. Mu, X. Wang, *Chem. Commun.* **2012**, *48*, 7350.
[131] H.-Y. Zhu, Y.-Q. Fu, R. Jiang, J. Yao, L. Xiao, G.-M. Zeng, *Bioresour. Technol.* **2012**, *105*, 24.
[132] G. A. Mahmoud, *Monatsh. Chem. – Chem. Mon.* **2013**, *144*, 1097.
[133] Z. Yu, X. Zhang, Y. Huang, *Ind. Eng. Chem. Res.* **2013**, *52*, 11956.
[134] L. Jiang, P. Liu, *ACS Sustainable Chem. Eng.* **2014**, *2*, 1785.
[135] A. Konwar, A. Gogoi, D. Chowdhury, *RSC Adv.* **2015**, *5*, 81573.
[136] D. Zhang, P. Sun, P. Li, A. Xue, X. Zhang, H. Zhang, X. Jin, *Biomaterials* **2013**, *34*, 10258.
[137] K. Hu, J. Sun, Z. Guo, P. Wang, Q. Chen, M. Ma, N. Gu, *Adv. Mater.* **2015**, *27*, 2507.
[138] K. Kurd, A. A. Khandagi, S. Davaran, A. Akbarzadeh, *Artif. Cells, Nanomed., Biotechnol.* **2015**, DOI: 10.3109/21691401.2015.1008513.
[139] G. R. Mahdavinia, H. Etemadi, F. Soleymani, *Carbohydr. Polym.* **2015**, *128*, 112.
[140] C. H. Zhu, Y. Lu, J. F. Chen, S. H. Yu, *Small* **2014**, *10*, 2796.

